The role of the immune system in central nervous system neoplasia with a special focus on B cells

Dissertation

zur Erlangung des Grades eines
Doktors der Naturwissenschaften

der Mathematisch-Naturwissenschaftlichen Fakultät
und
der Medizinischen Fakultät
der Eberhard-Karls-Universität Tübingen

vorgelegt
von

Constanze Louisa Kemmerer
aus Heppenheim, Deutschland

2023

Tag der mündlichen Prüfung: 28.03.2023

Dekan der Math.-Nat. Fakultät: Prof. Dr. Thilo Stehle
Dekan der Medizinischen Fakultät: Prof. Dr. Bernd Pichler

1. Berichterstatter: PD Dr. Markus Kowarik

2. Berichterstatter: Prof. Dr. Ulrike Naumann

Prüfungskommission: PD Dr. Markus Kowarik

Prof. Dr. Ulrike Naumann

Prof. Dr. Jens Schittenhelm

Prof. Dr. Karin Schilbach

Erklärung / Declaration:

Ich erkläre, dass ich die zur Promotion eingereichte Arbeit mit dem Titel:

„The role of the immune system in central nervous system neoplasia with a special focus on B cells“

selbständig verfasst, nur die angegebenen Quellen und Hilfsmittel benutzt und wörtlich oder inhaltlich übernommene Stellen als solche gekennzeichnet habe. Ich versichere an Eides statt, dass diese Angaben wahr sind und dass ich nichts verschwiegen habe. Mir ist bekannt, dass die falsche Abgabe einer Versicherung an Eides statt mit Freiheitsstrafe bis zu drei Jahren oder mit Geldstrafe bestraft wird.

I hereby declare that I have produced the work entitled “The role of the immune system in central nervous system neoplasia with a special focus on B cells”, submitted for the award of a doctorate, on my own (without external help), have used only the sources and aids indicated and have marked passages included from other works, whether verbatim or in content, as such. I swear upon oath that these statements are true and that I have not concealed anything. I am aware that making a false declaration under oath is punishable by a term of imprisonment of up to three years or by a fine.

Tübingen, den ....

Datum / Date Unterschrift /Signature

Contents

Acknowledgements

I would like to express my deepest appreciation to PD Dr. Markus Kowarik for the supervision of this dissertation and his invaluable feedback and input.
I am further extremely grateful to Prof. Dr. Ulrike Naumann for her generously provided knowledge and expertise and her openness to give guidance and support during the last four years.
I could not have undertaken this journey without the generous help of Prof. Dr. Jens Schittenhelm who always supported new ideas, openly shared his knowledge and provided precious feedback.
Words cannot express my gratitude for Matthias Scholl, Evelyn Dubois and the whole technician team of the Neurolabor at the University Hospital in Tübingen. This dissertation would not have been possible if it was not for their dedication to teach me new methods and provide me with their expertise and knowledge as well as their emotional support.
Special thanks should also go to the study nurses Ulrike Baumann and Natalie Rumpel for their professional as well as emotional support.
I would like to extend my sincere thanks to the coauthors of the first study who open-mindedly supported this project in many different ways.
Additionally, I had the pleasure of working with Deniz Bulgur, Célia Hinrichs and Laura Neumann who completed their theses in parts of my project. I am grateful for their dedication to the project and the inspiring discussions we had.
I would also like to acknowledge the friendly and supportive working environment created by all members of the laboratory and the willingness of all study participants to contribute to this project.
Further I would like to thank the Graduate Training Center for Neuroscience in Tübingen for their time and effort to support and guide me during the past 6 years.
Many special thanks go to my friends who always had my back and supported me in so many different ways. I would especially like to recognize Alexander Conzelmann's help in python coding for some of the analyses.
Lastly, I would like to express my deepest gratitude to my family and especially my parents. Without their continuous motivation and feedback this work would not have been possible.

Abstract

Introduction: Cancer is one of the leading causes of death worldwide. While there are high hopes on immunotherapy to treat tumors, the roles of individual cell types contributing to the immunotherapeutic success are still incompletely understood. This dissertation is mainly concerned with the role of leucocytes – with a special focus on B cells. Understanding B cell function in anti-tumor immunity and their interaction with the microenvironment may help improve cancer therapy. Therefore, in the first part, leucocyte infiltration in the most common malignant primary brain tumor is assessed and associated with the immunological tumor milieu. In the second part, the role of cerebrospinal fluid (CSF) B cells is determined, the scope of their antibody dependent immunity is assessed and antigen targets are identified.

Methods: In study 1, tumor tissues of 18 glioma patients (14 glioblastomas (GBM), 4 astrocytomas grade III (AA)) were stained for leucocyte infiltration by immunohistochemistry. Lymphocytes (CD45+), total macrophages (CD68+) and alternatively activated pro-tumor macrophages (CD163+) were identified and their relative contribution to the immune cell composition was determined. Additionally, the levels of 30 cytokines were measured in the CSF of the respective patients, compared to non-inflammatory controls and correlated with the immune cell infiltration pattern. In study 2, the B cell repertoire of three meningeosis neoplastica patients was determined from CSF B cells by single cell sequencing. Clonal expansion was analyzed and recombinant antibodies were produced for some clones. Circulating antibodies in blood and CSF were measured by mass spectrometry and resulting peptide sequences were compared to the CSF B cell repertoire. Moreover, a blood B cell repertoire was generated by next generation sequencing and screened for clonally related cells to the CSF B cell repertoire. Lastly, recombinant antibodies produced from CSF B cells were used to determine tumor specificity and antigen targets. Therefore, recombinant antibodies were used to stain primary fibroblasts of a healthy control subject and a malignant fibroblast cell line by flow cytometry and binding against target antigens was assessed by a protein microarray and enzyme linked immunosorbent assays (ELISAs).

Results: In study 1**,** macrophage infiltration was prominent in the glioma tissue, but lymphocyte infiltration was low. For CD45+ lymphocytes as well as for CD68+ macrophages infiltration was higher in perivascular tissue than in the tumor core. CSF of glioblastoma patients showed a decreased level of interleukin-7 compared to controls and a tendency towards higher levels of interleukin-2, interleukin-6 and vascular endothelial growth factor. Additionally, CD68+ macrophages were negatively correlated with eotaxin, interferon-γ, interleukin-1β, interleukin-2, interleukin-10, interleukin-13, interleukin-16, vascular endothelial growth factor and the inflammatory cluster component derived by factor analysis. In study 2, CSF B cells were clonally expanded and overlapped with antibody sequences from CSF and serum. No clonal relation could be determined to the blood repertoire. Flow cytometric data showed similar staining patterns for healthy and malignant cells. Screening of recombinant antibodies against the protein microarray produced a large hit list with no clear cut results, but subsequent ELISAs uncovered relevant staining of various antibodies against DDX53, some marginal staining of recombinant antibody F1-P3 against AKR1A1and MTUS2 and some marginal staining of recombinant antibody B8-P1 against AKR1A1, MTUS2 and ACY3 as well as F6-P1 against MTUS2.

Conclusion: Lymphocyte levels in gliomas are low with macrophages being the major infiltrating leucocyte. Cytokine levels in the CSF of glioma patients appear to be dysregulated as in chronic inflammation. This may support tumor proliferation and growth by providing stimulating factors while protecting the tumor from immune attack. These cytokine levels are associated with immune cell infiltration and understanding the precise mechanisms of this interaction may help to induce an anti-tumor microenvironment increasing the efficiency of immunotherapies. In contrast, study two shows that CSF B cells in metastatic melanoma patients are clonally expanded and produce functional antibodies which can be found in serum and CSF. DDX53, a cancer testis antigen, was identified as a promising target for immunotherapy as it is hardly expressed in healthy somatic tissues. Additionally, since CSF B cell receptors bound this target, an immune response is likely to be triggered by this antigen. Identification of suitable targets for immunotherapy is critical for treatment efficiency in the future.

Cancer Immunology

General introduction to cancer development

The annual incidence of central nervous system tumors in the United States has been determined to be 23.41 per 100,000 in recent years and represents a significant health issue [1]. Standard treatment options seldomly lead to the desired effects and intense research is conducted in this field to improve overall survival and quality of life.

The development of a tumor has been associated with genetic risk factors, exposure to toxins as well as infection with biological pathogens [2]. Subsequent tissue destruction and immunogenic stimulation result in inflammation and dysregulation of the tumor microenvironment. It is estimated that up to 20% of cancers are preceded by infection, chronic inflammation or autoimmunity in the respective tissue since tumors can benefit from the release of inflammatory factors as well as trigger inflammatory responses themselves [3,4]. While during the last century the contribution of the immune system in tumor development has been strongly debated there is now a consensus that the immune system plays a significant role [5]. The original immunosurveillance model made the assumption that the immune system monitors and eliminates pathological changes of the tissue. However, nowadays this model has been expanded to also cover pro-tumoral effects of the immune system [5]. It is now divided into 3 phases – elimination, equilibrium and escape. The elimination phase recapitulates the immunosurveillance theory when the immune system successfully eliminates transformed cells and tumors may not even become clinically relevant. The equilibrium phase describes the containment of the tumor while complete elimination of pathogenic cells fails. In this phase the tumor also adapts to the immune response by e.g. becoming less immunogenic. In the last phase, the most sophisticated tumor cells are no longer captured by the host's immune response and start to grow heavily [5].

The tumor microenvironment includes a large variety of non-malignant cells including cells of the adaptive immune system but also cells of the innate immune defense like tumor associated macrophages, cancer associated fibroblasts, pericytes, adipocytes, myeloid-derived suppressor cells, tumor associated neutrophils, dendritic cells and vascular endothelial cells [6]. The precise mechanisms by which these cells constitute

pro or anti-tumorigenic effects is not yet completely understood. Here I want to summarize current knowledge on the potentially most relevant groups of cells for cancer.

T cells in cancer

The relevant role of T lymphocytes in cancer has been widely appreciated and assessed [7]. The association of T cell infiltrates with improved clinical outcome has been replicated for a variety of solid tumors – especially in the case of CD8+ T cells – while the influence of CD4+ and regulatory T cells has been less clearly defined [8]. The population of T cells is very heterogeneous, not only between different tumor entities but even within the same tumor as they may diverge from conventional T cell subsets, vary in degree and type of dysfunction as well as differ in the capacity to identify tumor antigens [7]. Tumor infiltrating T cells do not even necessarily need to be tumor specific, but can be solely bystander T cells [9]. Nevertheless, immunotherapies targeting T cells by checkpoint blockade have been successful at least in a subset of patients [10]. The rationale behind this therapy is the observation that prolonged exposure of T lymphocytes to their cognate antigen (e.g. in chronic infection) leads to an exhaustion profile of the respective T cells with the expression of inhibitory receptors and the loss of effector functions [7]. Antibodies against these inhibitory receptors have shown upregulation of the T cell response even though the effects may depend more on a replacement than a reinstatement of the exhausted tumor infiltrating T cells [11]. In addition, the tumor microenvironment may dysregulate T cells since they need to compete for nutrients with the demanding tumor and are constantly exposed to tumor metabolites [12] Even though more attention has been attributed to CD8+ T cell exhaustion, CD4+ T cell may also suffer from dysfunctional states in tumors [13] Results of studies analyzing the prognostic value of CD4+ T cells and regulatory T cells have however been somewhat contradictory [8].

B cells in cancer

In recent years also the role of B cells in tumor immunity has been appreciated and a large amount of research has been dedicated to identifying B cell signatures as biomarkers for survival and treatment response [14–16]. On the one hand, B cells are relevant for the humoral immune response by the production of anti-tumor antibodies [17]. On the other hand, B cells have many more tumor suppressive functions including

the capacity to promote T cells, to stimulate the immune system by cytokine release and also to directly lyse tumor cells [17]. On the contrary, B cells may also act as immunosuppressors in the tumor microenvironment by killing or inactivating anti-tumor T cells [18]. Consequently, studies analyzing B cell function in tumors have yielded varying results [16]. One of the major drawbacks in many studies is the lack of B cell subset identification to clarify the role of B cells in cancer development [19]. Especially the pro-tumoral role of regulatory B cells has been discussed. This B cell subset may reduce T cell antitumor responses by releasing immunosuppressive cytokines, the expression of checkpoint molecules and CD95-ligand induced T cell apoptosis [18,20]. An important question to be answered is to decipher which B cell subsets may acquire immunoregulatory capacity and how these cells can be identified [20,21].

Macrophages and cancer

Macrophages play important roles in the tumor microenvironment by regulating invasion, metastasis, angiogenesis, immunosuppression and therapy resistance [6,22–24]. While tissue resident macrophages were thought to reside exclusively from hematopoietic monocyte precursors there is now evidence for a significant contribution of embryonic-derived macrophages in a variety of tissues [25]. While the distinction of these cells by surface markers remains challenging, macrophages of different ontogeny may have distinct transcriptomic profiles as well as different life spans and functions [25]. However, macrophages in general can display very different phenotypes depending on their polarization. Classically activated macrophages (M1) are induced by interferon-γ and lipopolysaccharide. They secrete pro-inflammatory cytokines like interleukin(IL)-12, IL-23, TNF-α and IL-6 and stimulate Th1 responses [6,22,26,27]. Their high expression levels of major histocompatibility complex molecules makes them competent antigen presenting cells with strong tumoricidal capacity [24,26]. In contrast, alternatively activated macrophages (M2) are induced by IL-4, IL-10, IL-13 and transforming growth factor β (TGF-β). They activate Th2 cells and promote cell proliferation, tissue repair, angiogenesis and phagocytosis [6,22,26,27]. Macrophages can switch between the phenotypes based on environmental changes in cytokine and growth factor levels, hypoxia and other conditions [26]. Moreover, the phenotypes are not as clear cut as macrophages can have intermediate polarization stages and have been further differentiated into subgroups (e.g. M2a, M2b, M2c, and M2b) [26,28]. It

is assumed that at early stages of tumor initiation pro-inflammatory M1 macrophages predominate while at later stages macrophages are polarized towards the anti-inflammatory M2 type [28]. Regulating macrophage polarization remains to be an important research question also in regard to targeting macrophages as possible treatment options in cancer therapy [22].

Tertiary lymphoid structures and cancer

Tertiary lymphoid structures (TLS) are formations of immune cells which resemble secondary lymphoid organs [21]. They typically arise in inflammatory environments and are associated with positive prognostic outcomes in most solid tumors [15,21]. The precise mechanisms for better clinical outcomes and improved response to immunotherapies remains nebulous. Whether the unique cytokine milieu, the B cell T cell crosstalk or a combination of different factors contributes remains to be determined [15]. More precise classification of TLS concerning their immune cell composition and maturation level may specify prediction and possible targets for treatments [15].

Prospect

This dissertation presents results of two studies. The first study is concerned with identifying the composition of immune cells in glioblastoma and how they are related to CSF cytokine concentrations. The second study then more specifically evaluates the antibody-mediated immune response in B lymphocytes using a metastatic melanoma model.

The first study has been published and is openly accessible online [29]. Please note that all concepts, data, tables and figures presented in the following are taken from this publication if not indicated otherwise.

Characterization of the composition of the glioma microenvironment and associations with cerebrospinal fluid cytokine levels

Introduction

Glioblastoma

Among brain neoplasia, the most common type of malignant tumor is glioblastoma which has very low survival rates even when all approved treatment strategies are exploited [1,30]. Glioblastoma is believed to originate from neural stem cells (NSCs), NSC-derived astrocytes and oligodendrocyte precursor cells [31]. Since 2016, gliomas are no longer solely diagnosed on the basis of histological findings, but also genotype analyses are considered. Glioblastomas can thus be divided into 90% IDH-wild type comprising mostly primary glioblastomas and 10 % IDH-mutant glioblastomas corresponding mostly to secondary glioblastoma according to the previous definitions [32].

Glioblastoma has been defined as an immunologically “cold” tumor because of its lack of tumor antigens, the inability of antigen presenting cells to present antigens to effector cells and the low T cell activation [33]. Moreover, gliomas express high levels of immune checkpoint and suppressive factors causing an immunosuppressive tumor microenvironment [33]. In the next section, the fate of T cells, B cells and macrophages in the glioma microenvironment will be summarized.

T cells in glioma

While for some other cancer types there is evidence that lymphocyte infiltration correlates with overall survival, the influence of T cell infiltration in glioblastoma is still controversial [8,34]. The role of each T cell subset and their interactions need to be further analyzed for a better understanding of T cells in glioma [34]. General T cell dysfunction in glioma can be categorized into senescence, tolerance, anergy, exhaustion and ignorance [35]. Glioma supports this T cell dysfunction by releasing inhibitory cytokines, upregulating immune checkpoint proteins and impairing T cell migration [33]. Current immunotherapeutic approaches aim at activating dysfunctional CD8+ T cells [33]. In

contrast, regulatory T cells are considered tumor-promoting cells and have been associated with an immunosuppressive microenvironment and tumor growth promotion [36].

B cells in glioma

The relevance of B cells in glioma is also still not completely clear. B cells have been detected in tumor tissue in some patients but at relatively low levels below 5 % of all cells [37–39]. However, animal models have shown a significant survival benefit after local CD20 B cell depletion in the brain [37]. Moreover, recently, B cells were used in B cell based vaccines exploiting the antigen cross presentation ability and potential for immunological memory of these cells [40]. We therefore cannot yet exclude that B cells are a relevant immunological component in anti-glioma immunity.

Macrophages in glioma

Macrophages have been considered to be among the most important immune cells in the glioma microenvironment as they contribute up to 30-50 % of the total tumor mass [41–43]. Especially compared to the healthy brain gliomas show significantly higher macrophage infiltration [44]. These tumor associated macrophages (TAMs) are composed of about 85 % bone marrow derived infiltrating monocytes and approximately 15 % microglia, the brain resident macrophages [45]. Infiltrating macrophages seem to preferentially accumulate in perivascular areas while microglia can be predominantly found in peritumoral areas [45]. Further, only infiltrating TAMs have been associated with significantly lower overall survival in glioma and gene expression patterns seem to differ between the subpopulations [45,46] However, whether functional disparity between microglia and infiltrating macrophages exists still needs to be determined [47].

TAMs within the tumor are functionally, spatially and temporally heterogeneous [48]. So, not only the number but also the activation status may influence GBM prognosis [43]. Unfortunately, the polarization of macrophages, which has often been described as M1 or M2 type, is not as clear. Müller et al. could show that TAMs co-express M1 associated as well as M2 associated genes [46]. Nevertheless, there seems to be a

predominance of M2 macrophages in the tumor microenvironment [49]. Strategies targeting TAM recruitment, polarization and immune function have been developed and there is hope that TAM directed immunotherapy may improve glioma treatment [50].

CSF cytokines and their immunological effects in glioma

Cytokines are soluble molecules responsible for intercellular communication and regulate embryonic development, haematopoiesis and immune responses [51]. They not only influence the secreting cell but proximal and distant cell activity as well [51] and have been categorized into interleukins, growth factors, colony stimulating factors, interferons, tumor necrosis factors and chemokines [52]. Cytokines in cancer can have pro- as well as anti-inflammatory activity depending on the tumor microenvironment [52]. And even glioma cells themselves are capable of secreting these soluble factors regulating invasion, proliferation, migration, neo-angiogenesis and immune cell infiltration [53]. It is therefore not surprising that the regulation of cytokines has been researched in immunotherapeutic approaches [51].

Cytokines may induce a tumor friendly environment in different ways. Firstly, they can render T cells and other anti-tumorigenic cells dysfunctional, secondly, they can stimulate neo-angiogenesis, tumor invasion and growth and thirdly, they attract myeloid cells such as microglia and induce a tumor promoting phenotype in these cells [41,53,54]. Accordingly, also cytokines associated with T lymphocyte infiltration have been described with a special relevance for TGF-β [55–59]. While most studies have focused on cytokines in tumor tissue, less is known about the composition of these factors in the CSF of glioma patients. Surprisingly, Krzyszkowski et al. found decreased levels of the immunosuppressive factors IL-10 and TGF-β2 in the cerebrospinal fluid of glioma patients compared to controls [60]. Even though these results cannot yet be explained mechanistically, CSF is much easier to retrieve than tumor tissue and therefore CSF cytokine levels could be a good biomarker to estimate the immunological environment of the tumor in a non-invasive way. We therefore conducted a larger screening of CSF cytokine levels in glioma patients.

Research Goal

As described above, the role of lymphocytes – and especially B cells and tertiary lymphoid structures - in gliomas has not yet been conclusively determined. Moreover,

biomarkers to infer the composition and state of the tumor microenvironment from CSF are lacking. The first study therefore aimed at characterizing immune cell infiltrates in glioma patients, determining cytokine concentrations in the cerebrospinal fluid and analyzing the correlation between these two compartments.

Material and methods

Standard protocol approval and patients

The study was approved by the institutional review board of the University of Tübingen (ethics approval number 972/2018BO2). Patients were selected when 1) they had a confirmed diagnosis of IDH WT glioblastoma (WHO grade IV) or IDH WT anaplastic astrocytoma (AA, WHO grade III), 2) matching paraffin fixed tumor material and CSF of the same patient was available before initiation of radio- and chemotherapy, and 3) written informed consent was available for the usage of the biological material for research purposes. Samples of 18 patients matching these criteria were kindly provided by the biobank of the Center for Neuropathology and the biobank of the Hertie Institute for Clinical Brain Research (HIH) in Tübingen. CSF of age and gender matched non-inflammatory controls (4 patients with cognitive deficits, 5 patients with affective disorder, 2 patients with normal pressure hydrocephalus, 1 patient with migraine, and 2 healthy controls) was kindly provided by the biobank of the Hertie Institute for Clinical Brain Research (HIH) in Tübingen.

Handling of tumor material

Paraffin embedded tissue was sliced at a thickness of 4 µm and mounted onto glass slides. The tissue was processed by the Institute for Neuropathology in Tübingen in line with the routine diagnostic workflow. In short, hematoxylin and eosin staining was done for each sample to control for tumor content. Immune cells were stained on an autostainer (Ventana Benchmark IHC optiView System (Roche, Ludwigsburg, Germany)) using mouse anti human CD68 (Dako, PGM-1, 1:1200) and mouse anti human CD163 (AbD Serotec, cloneEDHu-1, 1:1000) for macrophage detection and mouse anti human CD45 (Dako, clone 2B11, 1:1200) for leukocyte screening. Tonsil was stained as a positive control.

MGMT status was taken from results of the routine diagnostics of the University Hospital in Tübingen as assessed by the Institute of Neuropathology. In short, 250 ng genomic DNA isolated from the tissue was pyrosequenced using BlackPREP FFPE Kit (Analytik Jena, Germany). After bisulfite conversion using the Promega MethylEdge Bisulfid Conversion System (Promega, Madison, WI, USA) according to the manufacturer's protocol, PCR amplification and pyrosequencing covering the five CpG islands 74–78 in exon 1 of the MGMT locus on chromosome 10q26 were performed with the PyroMark Q24 CpG MGMT kit (Qiagen). Classification was achieved by using the mean percentage of methylated alleles at all five CpG loci and applying established cut-offs (< 8 % versus > 8 % methylation level).

Cytokine concentrations in CSF

To determine the cytokine concentrations in the CSF the V-PLEX Human Cytokine 30-Plex Kit (Meso Scale Diagnostics) and the Human CXCL13/BLC/BCA-1 DuoSet ELISA (R&D) were used according to the manufacturer's protocols. The multiplex assay was measured on the Sector Imager 6000 (Meso Scale Diagnostics, Rockville, MD, USA) while the CXCL13 ELISA was measured on the Sunrise Reader (TECAN, Crailsheim, Germany). In case enough material was available samples were measured in duplicates (see Table 1). Additional CSF parameters for the subjects were retrieved from the SAP system at the University Hospital Tübingen.

IHC data analysis

Tumor slides were analyzed at 200x magnification using a light microscope with a Progres C10 camera system (JenOptik, Germany). To cover the large intratumoral diversity of some tumors, for every staining the same region of the tumor was analyzed. A minimum of 3 different tumor areas for homogeneous tissue and at least one image of each morphologically different area (minimum of 3 in total) for heterogeneous tissues was considered. Subsequently, photomicrographs were classified by a board-certified neuropathologist (Prof. Schittenhelm) into "core tumor" or "infiltration zone". Additionally, the perivascular region was determined for each tumor in the 50 µm radius around 2 large vessels (> 5 µm) respectively (Fig. 1). Stained cells were counted manually using QuPath Software Version 0.2.1 (University of Edinburgh, UK) and calculated as both percentage of cells relative to overall stained nuclei as well as absolute number of cells per mm^2.

Statistical Analysis

Cytokine data was assessed using MSD Discovery Workbench software 3.0 (Meso Scale Diagnostics, Rockville, MD, USA). Statistical analyses were conducted using SPSS (IBM SPSS Statistics Version 25.0 for Windows, IBM Corportion, Armonk, NY,

Table 1 Data Cleaning

	% Samples set to highest Standard	% Samples set to 0	% of duplicates
Eotaxin			93.54
Eotaxin-3			93.54
IP-10	6.25		93.54
MCP-1	31.25		93.54
MCP-4			93.54
MDC			93.54
MIP-1α			93.54
MIP-1β			93.54
TARC			93.54
M-CSF		87.5	93.54
IL-12p40			93.54
IL-1α		78.13	93.54
IL-1β		18.75	19.35
IL-2		6.25	19.35
IL-4		65.63	19.35
IL-5		28.13	93.54
IL-6			19.35
IL-7			93.54
IL-8			93.54
IL-10			19.35
IL-12p70		59.38	19.35
IL-13		37.5	19.35
IL-15			93.54
IL-16			93.54
IL-17		96.88	93.54
TNF-α		3.13	19.35
TNF-β		96.88	93.54
VEGF	3.125	3.13	93.54
IFN-γ		54.4	19.35
CXCL13		100	100

Table 1: Data cleaning of the cytokine concentrations for all subgroups. Samples exceeding the detection limit were set to the highest standard while samples below the detection limit were set to zero. Percentages of these cases are presented. Additionally, samples were run in duplicates when enough material was available. Percentages of these cases are shown. The table was taken with permission from Kemmerer and colleagues [29]

USA). and graphs were designed using GraphPad Prism (Version 8 for Windows, GraphPad Software, San Diego, California USA). Since the Kolmogorov-Smirnoff-test showed significant deviations from normality ($p < 0.5$) nonparametric tests were used.

The difference in absolute and relative immune cell infiltration between AA and GBM in tumor core and perivascular area was assessed by the Mann-Whitney-U test. Differences between tumor core and perivascular area within the same patients were calculated using the Wilcoxon-rank-test. Likewise, differences to the tumor core were determined for samples containing an infiltration area. To compare the three immune stainings the Kruskal-Wallis-Test was used.

Since some cytokine measurements exceeded the limits, the values exceeding the upper limit of detection (ULoD) were set to the highest standard, while values below the lower limit of detection (LLoD) were set to zero. Variables with less than 5 values per group above the LLoD including CXCL-13, GM-CSF, IL-17, IL-1α, TNF-β and IL-4 were excluded for the analysis. For duplicate measurements the mean was used for analysis and only comparisons between controls and GBM patients were assessed using Mann-Whitney-U test, since controls were only age and gender matched for the latter and not for AA.

To structure the data a principal component analysis was conducted using data from all groups including AA. CXCL-13, GM-CSF, IL-17, IL-1α and TNF-β had to be excluded from the analysis due to low variance while MCP-1, IL-5, IL-7 and VEGF were removed due to low sampling adequacy (Kaiser-Meyer-Olkin, KMO, value < 0.5). Regression factor scores were saved and compared among all three subject groups using the Kruskal-Wallis-Test.

Lastly, GBM cytokine concentrations and factor scores were correlated with immune cell stainings. Differences in cytokine concentrations and immune cell infiltrates were assessed for MGMT methylation status and sex using the Mann-Whitney-U test. Also, correlations of immune cell infiltrates with patient age and overall survival (defined as days until death or if unknown until last entry in the SAP system at the time of data retrieval) were calculated. Again, CXCL-13, GM-CSF, IL-17, IL-1α, TNF-β and IL-4 were removed from these analyses due to low variance.

To balance false positive mistakes and detectability the p-value for statistical significance was set to $p < 0.01$ for all tests.

Results

Sample characteristics

Mean age of all subgroups was 63 years. Mean overall survival in the GBM group was 386 days while the AA group had a mean overall survival of 183 days. In the GBM and control groups 36 % of patients were female and 64 % male, whereas in the AA group 50 % were male and female, respectively. In both AA and GBM groups blood brain barrier disruption was noticed in 50 % of the patients. Lastly, 50 % of the GBM patients and 25 % of the AA patients showed a MGMT promotor methylation. For a detailed overview on patient and control group characteristics see Table 2 and Table 3 respectively.

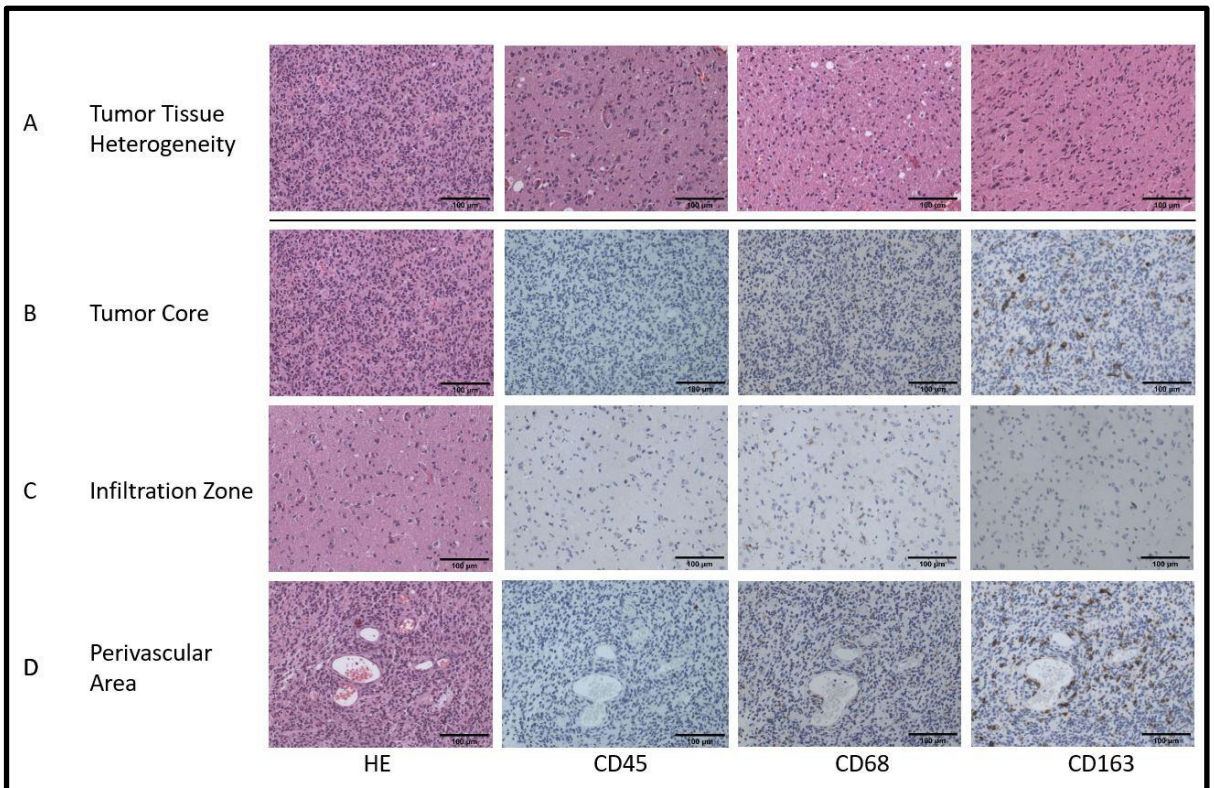

Fig. 1 Immunohistochemical staining of glioma tissue. The figure shows representative microscopic images of one glioblastoma patients at 200x magnification. We stained with hematoxylin and eosin (first column), anti-CD45 (second column), anti-CD68 (third column) and anti-CD163 (fourth column). (A) demonstrates the morphological heterogeneity of the tissue, (B) the tumor core, (C) the infiltration zone, and (D) the perivascular area. The figure was taken with permission from Kemmerer et al. (2021).

Table 2 Patient Characteristics

Patient	Sex	Disease	MGMT status	Overall survival	Number of leucocytes	IgG Index	Albumin quotient	BBB disturbance	OCB
1	f	GBM	M	559	6	3.16	4.4	no	2
2	f	GBM	M	49	1	0.36	7.4	no	1
3	m	GBM	M	1387	1	0.62	20.9	yes	1
4	f	GBM	M	335	3	0.54	18.8	yes	1
5	m	GBM	U	126	1	0.44	10.4	yes	N.A
6	f	GBM	U	308	1	0.44	2.5	no	1
7	m	GBM	U	522	4	0.78	44.8	yes	4
8	m	GBM	U	689	1	0.46	2.6	no	N.A
9	m	GBM	U	24	3	0.52	12.8	yes	1
10	m	AA	U	38	1	0.48	22.5	yes	4
11	m	GBM	U	323	6	0.52	11.6	yes	1
12	m	GBM	M	108	1	0.5	5.8	no	1
13	f	GBM	M	96	2	0.51	6.7	no	4
14	m	AA	U	600	4	0.47	5.9	no	1
15	f	AA	U	79	1	0.49	8.3	yes	N.A
16	f	AA	M	14	1	0.46	5.0	no	1
17	m	GBM	U	13	6	0.43	8.0	no	5
18	m	GBM	M	867	1	0.52	10.7	yes	1

Table 2: Demographic and cerebrospinal fluid characteristics of high grade glioma (HGG) patients are displayed. Overall survival is presented in days and number of leukocytes is presented in cells per µl CSF. All HGG are isocitrat-dehydrogenase wildtype gliomas. Abbreviations: f: female, m: male, MGMT: O6-Methylguanin-DNA-Methyltransferase, IgG Index: immunoglobulin G index, BBB: blood brain barrier, OCB: oligoclonal bands with numbers referring to OCB type: 1: no OCB visible in serum and CSF, 2: OCB only visible in CSF and not in serum, 3: OCB exclusive to CSF and additionally identical OCB in serum and CSF, 4: identical OCB in CSF and serum, 5: paraprotein split into closely adjacent bands, GBM: glioblastoma, AA: astrocytoma grade III, M: methylated MGMT promotor, U: unmethylated MGMT promotor, N.A.: not available. The table was taken with permission from Kemmerer and colleagues [29].

Immune cell infiltration between tumor areas

In a first analysis we evaluated differences in CD45+ leucocyte, CD68+ macrophages and CD163+ M2 type macrophages in tumor core, perivascular area, and infiltration zone (Figs. 1 and 2). Except for a trend towards higher CD163+ macrophage infiltration in GBM tumor tissue (U=5, p =0 .012) no significant differences could be found in the percentage or the absolute count between AA and GBM. We therefore combined AA and GBM groups into one high grade glioma (HGG) group for further analyses.

Comparing absolute cell counts in the different tumor areas among each other CD45+ leukocytes had a significantly lower count than CD68+ macrophages in all three tumor

Table 3 Characteristics of control subjects

Patient	Sex	Disease	Number of leucocytes	IgG Index	Albumin quotient	BBB disturbance	OCB
19	m	Healthy	3	N.A.	N.A.	N.A.	N.A
20	m	Cognitive deficit	2	2.3	4.8	no	N.A
21	f	NPH	N.A.	N.A.	N.A.	N.A.	N.A
22	m	Cognitive deficit	1	0.45	6.9	no	N.A
23	f	NPH	1	0.47	5.9	no	N.A
24	m	Healthy	1	0.51	5.5	no	N.A
25	m	Bipolar disorder	1	0.47	5.7	no	N.A
26	f	Cognitive deficit, Depression	5	0.5	14.5	Yes	N.A
27	f	Migraine	2	0.45	8.2	yes	N.A
28	m	NPH	1	0.41	4.6	no	N.A
29	m	Bipolar disorder	1	0.52	7.1	no	N.A
30	m	Episode of Depression	1	0.51	4.9	no	N.A
31	m	Depression	<1	0.39	13.3	no	N.A
32	f	Cognitive deficit	1	0.50	7.2	no	N.A

Table 3: Demographic and cerebrospinal fluid characteristics (CSF) of the control group are displayed. Number of leukocytes is presented in cells per µl CSF. Abbreviations: f: female, m: male, NPH: normal pressure hydrocephalus, MGMT: O6-Methylguanin-DNA-Methyltransferase, IgG Index: immunoglobulin G index, BBB: blood brain barrier, OCB: oligoclonal bands, N.A.: not available. The table was taken with permission from Kemmerer and colleagues [29].

areas ($p < 0.001$ for all comparisons) and additionally a significantly lower number of CD45+ cells compared to CD163+ M2 type macrophages in the tumor core ($p = 0.06$) (Fig. 2A/ C). When comparing the immune cell infiltrates between the different tumor areas, CD45+ and CD68+ cell numbers were significantly higher in perivascular areas compared to the tumor core ($p = 0.03$ for CD45+ cells and $p = 0.01$ for CD68+ cells, Fig. 2B/ C). Further, there was a tendency towards higher CD68+ and CD163+ macrophage infiltration in the tumor core in contrast to the infiltration zone which did not reach statistical significance ($p = 0.017$ for CD68+ macrophages and $p = 0.012$ for CD163+ M2 like macrophages, Fig. 2B/ C).

Looking at the percentage distribution of immune cell infiltrates, the percentage of CD45+ cells (tumor core: median 1 %, mean: 4 %; perivascular area: median: 3 %, mean: 7 %; tumor infiltration zone: median: 3 %, mean: 3 %) was significantly lower

than the percentage of CD68+ cells (tumor core: median 19 %, mean: 22 %; perivascular area: median: 27 %, mean: 27 %; tumor infiltration zone: median: 19 %, mean: 21 %) within the tumor core ($p < 0.01$), perivascular area ($p < 0.01$) and tumor infiltration zone ($p = 0.01$). Further, within the tumor core the percentage of CD163+ cells (median: 9 %, mean: 12 %) was significantly higher than the percentage of CD45+ cells ($p = 0.006$). When looking at the difference in the percentage of immune cells between the different tumor areas, percentages of CD45+ cells were significantly higher in the perivascular area compared to the tumor core ($p = 0.008$). Moreover, there was a trend towards increased percentages of CD68+ macrophages in the perivascular area compared to the tumor core ($p = 0.02$).

Differences in cytokine concentrations and principal component analysis

In a next step, cytokine concentrations in the CSF were measured and compared between GBM and control groups (Fig. 2D). GBM patients showed a significantly lower IL-7 level ($U = 41$, $p=0.009$) and a tendency towards higher IL-2, IL-6 and VEGF concentrations ($U = 48.5$, $p = 0.02$; $U = 46$, $p = 0.017$; $U = 54$, $p = 0.043$, respectively). To study the cytokine pattern we conducted a principal component analysis (PCA) which yielded an overall sampling adequacy of Kaiser-Meyer-Olkin-criterion (KMO) = 0.783 with a KMO > 0.5 for the individual items and sufficiently large correlations as assessed by the Bartlett's test of sphericity ($X2 (210) = 1127.002$, $p < 0.001$). Kaiser's criterion (eigenvalues >1) supported a 5 component solution explaining 93% of the variance. However, visual evaluation of the scree plot suggested a 2 factor solution which still explained 80% of the variance. Since the sample size was relatively small the two factor solution was chosen for further analysis. Because correlations between variables were expected, the Promax oblique rotation method was used and resulted in a factor correlation of $r = 0.605$. The extracted components overlapped with the initial categories "chemokines" (component 1, including primarily MIP-1α, MIP-1β, eotaxin, eotaxin-3. IP-10, MDC, MCP-4, TARC, IL-8, IL-6 and IL-12p40) and "cytokine panel" and "proinflammatory panel" (component 2, including primarily IFN-γ, IL-4, IL-12p70, IL-2, IL-16, IL-13, IL-1β, IL-10 and TNF-α) of the original V-PLEX scales. Accordingly, components were named "chemokines" and "inflammatory cluster". Regression factor scores were then compared between GBM, AA and controls which did not show any significant effects.

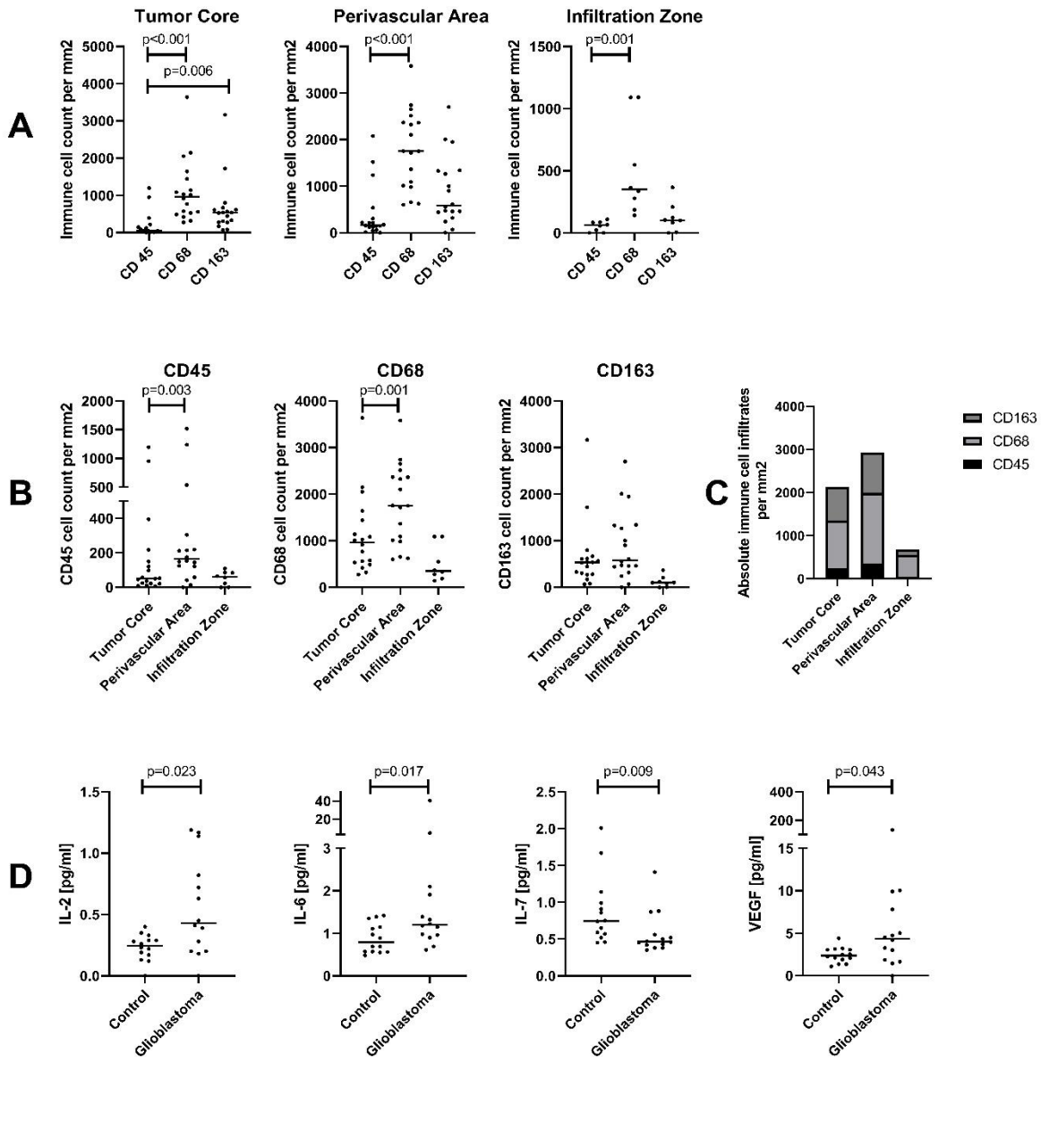

Fig. 2 Differences in immune cell infiltration and cytokine concentrations. (A) shows the differences in the infiltration of CD45+, CD68+ and CD163+ cells (median cell counts per mm^2) within each defined tumor area. (B) illustrates the differences in infiltration (median cell counts per mm^2) between the different tumor areas. (C) gives an overview on the distribution of immune cell infiltrates (median cell counts per mm^2) separated by tumor area. (D) shows the median concentrations (inpg/ml) of IL-2, IL-6, IL-7 and VEGF in the CSF for glioblastoma patients and controls. This figure was taken with permission from Kemmerer et al. (2021).

Correlation of immune cell infiltrations and cytokine concentrations

Immune cell infiltrates were correlated with the cytokine concentrations for GBM patients. Significant negative correlations could be found for CD68+ macrophages and

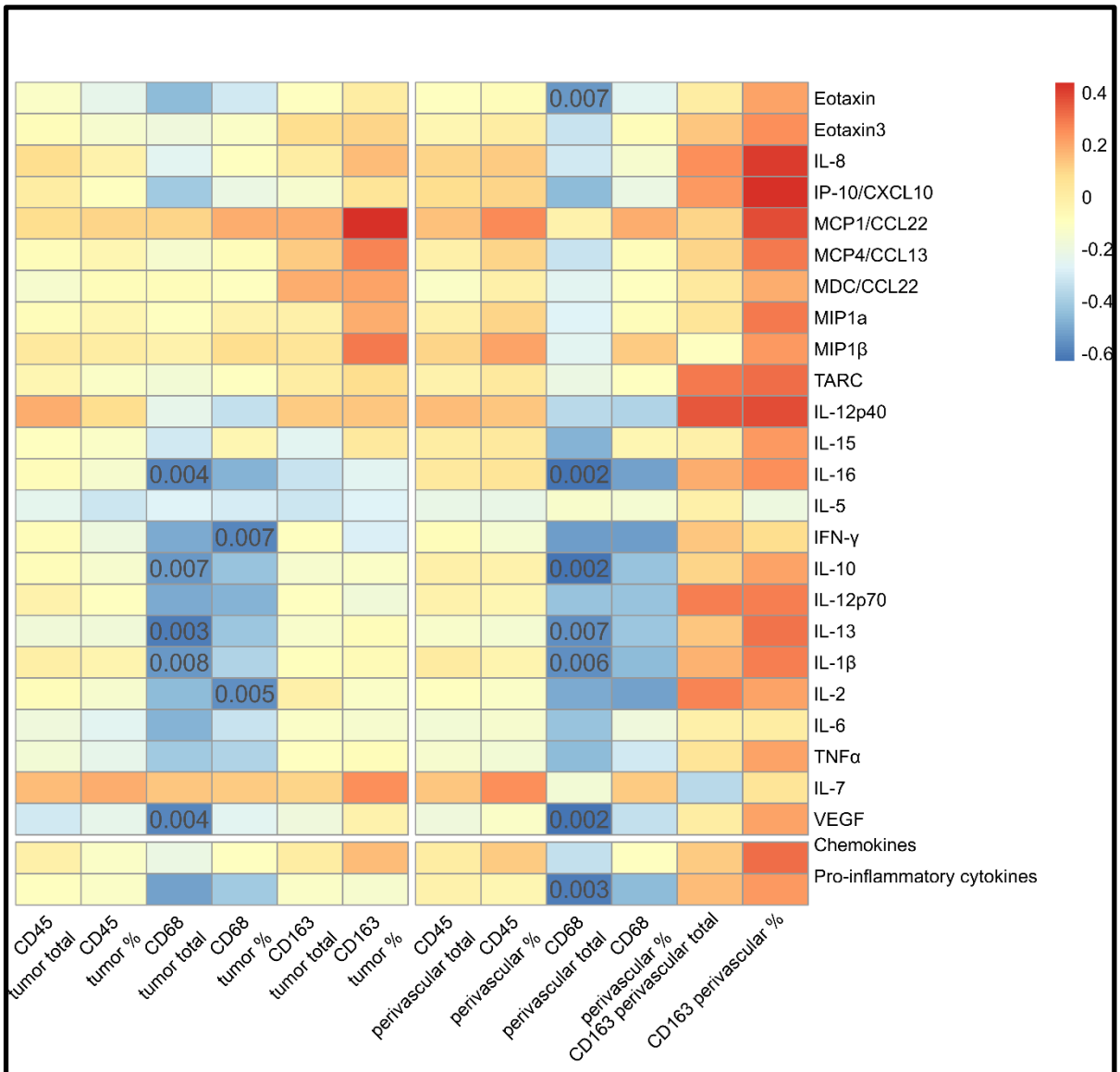

Fig. 3 Correlations between cytokines and immune cell infiltrates in the perivascular area. Correlations between CSF cytokines and regression factor scores of the principal component analysis with CD45+, CD68+ and CD163+ cells are displayed. Correlations have been calculated for relative and absolute immune cell counts in the perivascular area. Size and direction of the correlations are color-coded as indicated by the legend. Significant correlations are indicated with the respective p value in the matrix. This figure was taken with permission from Kemmerer et al. (2021).

concentrations of the cytokines eotaxin, IFN-γ, IL-1β, IL-2, IL-10, IL-13, IL-16, VEGF and factor score of component 2 (“Inflammatory Cluster”). Additionally, a trend towards a positive correlation of CD163+ cells in the perivascular area and IL8 and IP-10/CXCL10 and a trend towards a positive correlation of CD163+ M2 macrophages in

the tumor core and MDC-1/CCL22 (Fig. 3). For the cytokines showing significant correlations with CD68+ cells the differences in cytokine concentrations between GBM and controls are displayed in Fig. 4.

Half of the GBM patients had a disruption of the blood brain barrier (BBB) so a subgroup analysis was conducted to test if cytokine concentrations differed between these groups. Correlations of cytokine concentrations and immune cell infiltrates were also recalculated for these subgroups. There was no significant difference in cytokine concentrations, but almost all previously reported correlations failed to reach significance. Nevertheless, looking into the correlation plots revealed similar correlation patterns in both groups.

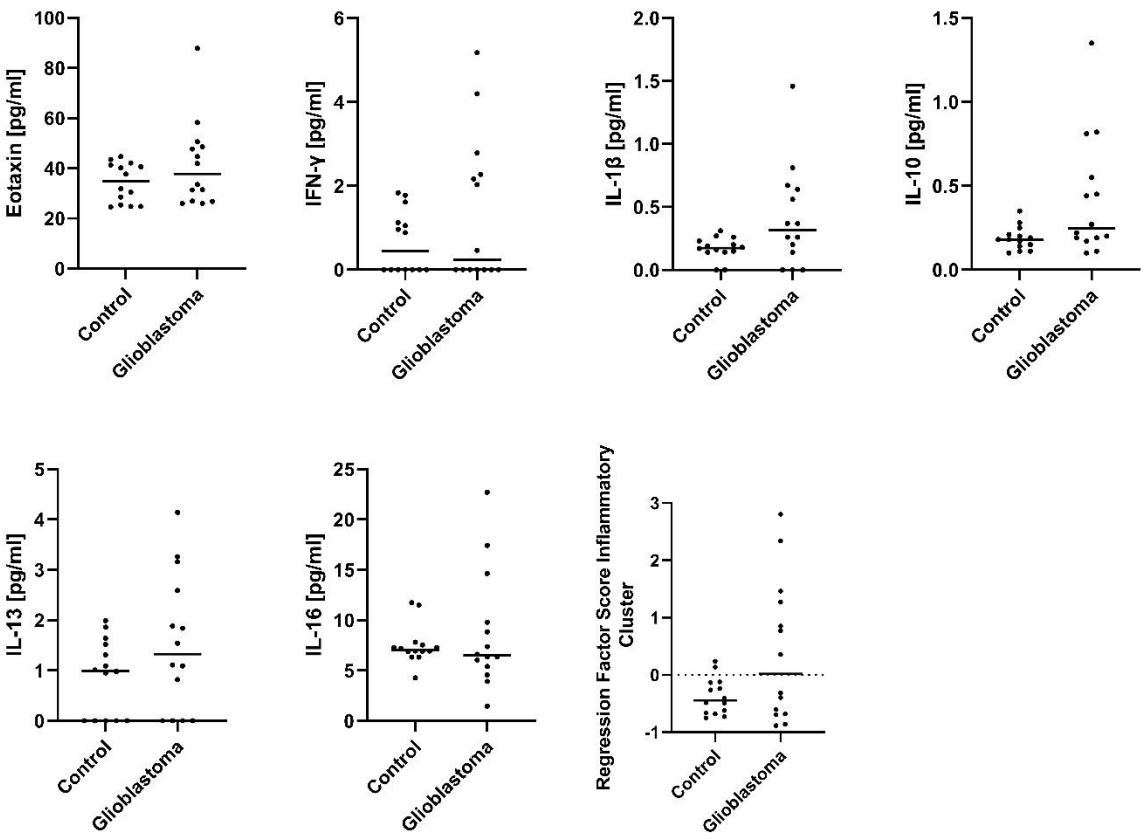

Fig. 4 Differences in cytokine concentrations. Comparison of cytokine concentrations and the regression factor score between GBM patients and controls for the cytokines and regression factor scores which had significant correlations with immune cell infiltrates. This figure was taken with permission from Kemmerer et al. (2021).

Effects of MGMT promotor methylation, sex, overall survival and age on immune cell infiltration and cytokine concentrations

MGMT promotor methylation had no effect on the cytokine concentrations, but there was a trend towards increased CD163+ M2 macrophages in the tumor tissue of patients with an unmethylated MGMT promotor region ($U = 7.00$, $p = 0.025$). There was no significant effect of sex on immune cell infiltration nor significant correlations of age and overall survival with immune cell infiltration and cytokine concentration.

Discussion

Results in context

In this study we assessed immune cell infiltration in HGG and the correlation with CSF cytokines. We found that lymphocyte numbers were lower compared to other brain tumor diseases [39] while macrophages were the major infiltrating immune cell type. In contrast to age and gender matched non-inflammatory controls, Il-7 was significantly lower in HGG while IL-2, IL6 and VEGF showed a trend towards higher concentrations in these patients. Regarding the correlations of immune cells and cytokines, CD68+ cells were significantly related to eotaxin, IFN-γ, IL-1β, IL-2, IL-10, IL-13, IL-16 and VEGF. Since the CSF has been considered a surrogate for pathophysiological changes in the central nervous system [61], we propose that CSF cytokine changes may affect cellular processes in the CNS. They may thus not only be relevant for clinical evaluation but also for therapeutic interventions.

B cells play a significant role in neuroinflammatory and other tumor diseases [62]. We therefore planned to analyze B cell counts in the CNS of HGG patients. However, we found even lower numbers of infiltrating leucocytes compared to previous reports [63,64]. Also, the B cell predicting factor CXCL13 was below detection limit in all samples. From this data we concluded that the role of B cells in HGG is limited. Thus, we did not continue to differentiate the leucocyte population into T and B cells.

We also compared the infiltration of leucocytes between the tumor core and the perivascular area and found the infiltration of leucocytes to be higher in the latter. Moreover, also macrophage infiltration was increased around blood vessels compared to the tumor core. One possible reason is the spatial proximity to the peripheral blood from where immune cells infiltrate the brain [65]. Brandenburg et al. assessed microglia and

macrophage infiltration in a mouse model of glioma and found an accumulation of these cells around blood vessel [66]. They are suspected to induce tumor angiogenesis by releasing proangiogenic factors. While our results are in line with this study, we determined only low numbers of macrophages with a pro-tumor M2 phenotype.

Lastly, we compared immune cell infiltration between infiltrative tumor areas and the tumor core. Macrophage numbers are higher in the core than the infiltration zone as supported by a study by Pinton et al. showing increasing numbers of macrophage infiltration from the periphery to the core [64]. Moreover, macrophages of the M2 phenotype were more prominent in GBM compared to AA. There is evidence for this effect also in microglia. Zhu et al. found that the expression of the purinergic receptor P2Y12 shifted from a cytoplasmic to a nuclear localization with increasing glioma malignancy grade and this shift was associated with the M2 marker CD163 expression [67].

Concerning the CSF cytokine concentrations IL-7 was significantly lower in HGG compared to controls. IL-7 can regulate T cell proliferation and survival [68,69] and has immune-reconstructive and activating properties in immunotherapy [70]. Moreover, it showed a survival benefit in an animal model when used in combination with IFN-γ [71]. Trends for elevated cytokine concentrations were determined for the proinflammatory cytokines IL-2 and IL-6 and the angiogenic factor VEGF. An upregulation of the latter two cytokines in glioma has been described previously [72–75]. IL-6 has additionally been associated with macrophage infiltration [76].

Taken together only minor changes in cytokine levels were observed. The low infiltration of lymphocytes differentiates HGG from other brain tumor entities such as metastatic disease [77,78]. It thus seems that immunosurveillance in HGG is limited.

Despite these small changes, we nevertheless found correlations for cytokine concentrations and immune cell infiltrations. CD68+ macrophages negatively correlated with the inflammatory cluster factor derived from the principal component analysis. In detail this included significant negative correlations with eotaxin, IFN-γ,IL-1β, IL-2, IL-10, IL-13, IL-16, and VEGF. Among these, IL-2 and VEGF showed a tendency towards increased levels as described previously, IL-13, Il-10 and IL-1β showed only minor increases compared to controls while there were no effects seen for the remaining cytokines. A detailed description of the cytokines associated with CD68+ macrophages

and their involvement in the pathophysiology of glioma can be found in the publication of the study presented here [29].

While some of the cytokines correlating with CD68+ macrophages have been associated with the M2 phenotype in the literature [79] we only found trends towards a positive correlation of CD163+ cells and IL-8, IL-10 and MDC-1. The small sample size and the rather conservative alpha error correction may be responsible for this finding.

For most cytokines correlating with macrophage infiltration we found evidence for their involvement in glioma pathology. Nevertheless, we only conducted correlative analyses and cannot directly infer causal relationships. What is surprising is the negative association of the cytokines with macrophage infiltration. One explanation could be that cytokines are released in the proximity to the tumor and show a concentration gradient towards the CSF. An alternative explanation is that cells may further differentiate upon stimulation in the CSF. The change in surface markers may lead to the impression of a negative association. Indeed, we found some trends towards positive correlations of some cytokines with the M2 phenotype identified by the CD163 surface marker.

Because the disturbance of the (BBB) in some patients may have affected the tumor microenvironment, we reconducted the correlation analysis with the subgroups. These showed the same trends indicating little relevance of the BBB disruption for the correlation of cytokine levels and immune cell infiltration. Additionally, the CSF / brain parenchyma barrier was previously considered a partial barrier [80] and may thus not drastically affect the microenvironment.

Lastly, MGMT methylation status while being discussed as a relevant factor in glioma prognosis [81] had no effect on the cytokine levels.

Whether the CSF truly reflects environmental circumstances in the tumor needs to be ultimately determined. However, taking the aforementioned evidence into consideration it is assumed that the CSF can be used as a surrogate after the exact immunological mechanisms in glioma patients have been identified.

In summary, the role of cytokines in glioma pathology is ambiguous. On the one hand cytokines help the immunosurveillance which is responsible for suppressing the outgrowth of abnormal cells. At the same time cytokines can cause chronic inflammatory states which promote cancer [3,82]. The exact mechanisms of glioma development are not fully understood, but they finally lead to a dysregulated immune state with the existence of pro- and anti-inflammatory factors in parallel [83]. This “immune chaos” may eventually lead to tumor progression and invasiveness. Pro-inflammatory cytokines may help cell survival, proliferation, migration and angiogenesis [84] while immunoregulatory factors such as IL-10 protect the tumor against clearance by the immune response [53].

Macrophages have been attributed a key role in cancer immunity due to their pro- or anti-inflammatory differentiation capacity [79]. Understanding the processes that trigger the differentiation into a specific direction may thus offer valuable targets for immunotherapy.

Limitations

A few limitations need to be pointed out. Firstly, due to limited material availability of the tumor tissue we did not conduct immunohistochemical dual staining. It would have been interesting to confirm that all CD163+ cells belonged to the macrophage (CD68) family. Since a specific surface marker staining for macrophages is not commonly agreed on we used the staining we found most commonly used in the literature and only identified all macrophages and the M2 subtype as described previously [4,85,86]. A further differentiation of macrophage subgroups by mRNA or protein expression may be useful to better characterize the macrophage interactions with cytokines and identify potential immunotherapeutic targets.

Secondly, the sample size of the study was rather small. Unfortunately, only little material was available for matched CSF and tumor tissue. This is also why we did not conduct longitudinal analyses even though it would have been interesting to trace immunological changes after radio- and/or chemotherapy. Additionally, non-healthy participants had to be included in the control group since lumbar punctures in healthy individuals are rare. Nevertheless, subjects in the control group were screened carefully to make sure that only subjects with noninflammatory conditions were included.

Thirdly, it cannot be excluded that cytokine measures were biased due to the measurement of 10 cytokines in parallel. This may not have allowed an optimal dilution of the individual factors. However, we conducted the multiplex assay according to the manufacturer's instructions.

Lastly, the overall survival of the AA group was lower than in the GBM group. This is surprising but may be explained by the very small number of AA patients and a relatively long survival of single patients.

Evaluation

Determining immune cell infiltration in the tumor tissue of glioma patients showed very low to absent levels of lymphocytes while macrophages are the most represented immune cell type in our analyses. This supports the notion of an immunological cold tumor with very little influence of B cells at least in the untreated disease condition. Additionally, the tumor microenvironment presents with a dysregulated cytokine profile resembling a state of chronic inflammation which may support tumor progression. Further goals to pursue are therefore finding strategies to increase lymphocytes in the brain parenchyma by immunotherapies or to determine the mechanisms to control anti-tumor effects in macrophages which are already present. Based on our finding that macrophages correlate with CSF cytokines, the latter could be identified with clearly defined cytokine signatures in the CSF after macrophage subsets have been more stringently analyzed.

After identifying some of the key components of the tumor microenvironment in glioma, the second study deals with antibody-mediated immune responses of B cells in metastatic melanoma patients to more specifically determine the role of B lymphocytes in tumor immunology.

Do B cells in the CSF of metastatic melanoma patients reflect an immunological response against the tumor?

Introduction

B cells in cancer

The CNS has long been considered an immune-privileged organ as defined by the incapability to induce an immune response after experimental implantation of a tissue graft [87]. However, afferent and efferent connections to the external immunity exist [87]. Under certain conditions, the limited immune cell trafficking between the CNS and the periphery can further be modulated. Following antigen exposure, T cells induce the release of inflammatory cytokines which can change the characteristics of the blood brain barrier enabling increased immune cell infiltration [87]. It is thus of great interest to characterize the immune cell infiltration in cancer.

Next generation sequencing of B cell receptors in cancer

Recent developments in high throughput sequencing analysis have opened a new field of studying cancer relevant immune reactions [88]. Since the lymphocyte repertoire diversity and distribution changes following acute as well as chronic diseases such as cancer, next generation sequencing (NGS) may help to understand the pathology and predict the disease course [89]. For example, Konishi and colleagues [90] used machine learning algorithms to differentiate between normal and tumor tissues and found distinct features between the samples. Moreover, repertoire analyses have been used to determine genes correlating with B and T cell expansion, preferred residues for somatic hypermutation and effector function associations with immunoglobulin (Ig) subsets [91].

The large diversity of B cell receptors in humans is due to the flexible arrangement of variable (V), diversity (D) and joining (J) immunoglobulin gene segments for heavy chains and V and J segments for the light chains [92]. Each antibody consists of two identical heavy and light chains and both participate in forming the complementarity determining regions (CDRs) where antibody antigen binding is determined [92]. Of these, the heavy chain CDR3 is the most variable region, since it is the section were

gene segments are joined [92]. Upon antigen contact somatic hypermutation can further diversify the antibody sequence to improve the match between antibody and antigen [92]. The somatic processes happening during B cell expansion especially in the CDR3 region makes B cell repertoire analysis a great tool to recover disease relevant immunological changes [92].

To determine endogenous antibodies both the specific heavy and light chain sequences of each antibody need to be determined. Zhang and colleagues [93] tried to overcome this difficulty by reassembling heavy and light chain sequences from mass sequencing based on statistical methods such as the co-enrichment of CDR3 regions. However, the authors admit that these do not necessarily reflect real endogenous antibodies, nor could they identify a surface protein as antibody target. Also, the B cell clone most expanded upon antigen encounter is not necessarily the most immunoprotective [92]. Mass sequencing may thus be a useful tool for understanding the cancer related immune reaction on a broader level, but does not seem to be a useful tool for therapeutic antibody development. Nevertheless, technological advancements making the sequencing of larger amounts of cells on a single cell basis more feasible can overcome this limitation [94,95].

CNS B cells in different diseases

In 2013, Kowarik and colleagues [96] analyzed the infiltration of B cells in patients with different diseases and found that in patients with neuroinflammatory diseases, B cell levels were elevated compared to healthy controls. Since hardly any B cell infiltration could be detected in healthy individuals, this indicates that these B cells are most likely related to the inflammatory condition. At the same time, slight increases in the percentage of CSF B cells could be found in some patients with metastatic brain disease and meningeal carcinomatosis [96]. It has been unclear whether these B cells arise due to an immune response against the tumor tissue.

Meningeosis neoplastica

Meningeosis neoplastica is the umbrella term for the metastatic spread of tumor cells into the subarachnoidal space and affects about 10% of patients with primary malignant tumors [97]. It is associated with changes of CSF parameters in some patients including elevated cell number, increased proportion of lymphocytes and presence of

immunoglobulins similar to other neuroinflammatory entities [98]. Kowaik and colleagues [96] could specifically show reduced CD4 T cells and elevated monocytes, NK cells and B cells in the CSF of some patients with meningeal metastatic spread. Since B cell numbers were virtually absent in healthy controls, this led to the assumption that CSF B cells may arise as a consequence of anti-tumor immunity.

Features of tumor associated antibodies

B cells in cancer can have antigen presenting functions with the capacity to induce T cell responses against the tumor [99]. Similarly, B cells can secrete functional antibodies against various cancer antigens which have been shown to be involved in both anti-tumor immune responses as well as tumor growth [100]. These antibodies, being accessible in a marginally invasive way, can serve as biomarkers for cancer detection and disease monitoring [100]. Moreover, they may aid the identification of immunological targets [100].

Antibody targets can be classified as tumor associated antigens (TAA), which describe auto-antigens which are either overexpressed or become exposed to the immune system [100]. Alternatively, tumor specific antigens (TSA) describe antigens which can be identified as non-self by the immune system because they contain mutation, deletions, or epigenetic modifications [100]. For an overview on common TAAs and TSA identified by autoantibodies see the review by de Jonge and colleagues [100].

To identify these antibody targets, immunoproteomic approaches have been used in the field [101]. Ganesan and colleagues [102] summarized the techniques used for autoantibody detection and based on this review some are outlined in the following.

A common technique is serological proteome analysis (SERPA) based on 2-dimensional electrophoresis (2-DE) separation of tissue or cell lysates. Patient samples containing autoantibodies are tested by their reactivity against the separated cell lysate proteins and are compared to equivalent healthy control samples. Proteins with unique reactivity against patient autoantibodies are excised and analyzed by mass spectrometry. However, proteins with certain physico-chemical properties cannot be identified using this technique.

Autoantibody mediated identification of antigens (AMIDA) is a different approach using immunoprecipitation to pull down potential autoantigens from tissue or cell lysates using patient autoantibodies bound to protein A or protein G beads. Captured proteins are then also analyzed by mass spectrometry. In some cases though, antibodies eluted with the proteins can mask the autoantigens making detection complicated.

A more recent method is the microarray based screening of autoantibodies. Antibodies of patient samples bind to arrays containing proteins or peptides of interest. Since these proteins are preselected, this method has the advantage that also low abundant proteins can be detected and post translational modifications can be incorporated in the assay.

However, tumor associated antibodies cannot only be identified on the protein level. B cell receptor sequencing of peripheral blood plasmablasts in metastatic cancer patients has been exploited to identify anti-tumor antibodies in these cells [103]. Peripheral blood plasmablasts showed clonal expansion and somatic hypermutation indicating an affinity maturation process against the target antigen. Additionally, similar paratopes could even be identified between different patients. Subsequently, recombinant antibodies derived from these plasmablast clones bound to non-autologous tumor tissue and tumor cell lines and even induced anti-tumor immune responses in mice. In a similar study, Rodriguez-Pinto and colleagues [104] used lymph node tissues of breast cancer patients to identify potential tumor associated antigens. Actively proliferating Ki67+ B cells showed somatic hypermutation and clonal expansion in the heavy chain variable domain. A recombinant antibody produced from these sequences was able to identify a cancer associated antigen by pulling down a protein from tumor extracts of the patient. Also, Pavoni and colleagues [105] analyzed tumor infiltrating B cells in breast cancer patients. B cells showed oligoclonality and specificity to 3 tumor surface antigens. Likewise, Bushey and colleagues [106] found B cell receptors against a conformationally distinct epitope of a cancer related autoantigen which were derived from memory B cells of lung cancer patients. A recombinant antibody produced from the retained heavy and light chain sequences successfully reduced tumor growth in vivo. These studies give evidence that tumor associated antigens seem to induce affinity maturation processes and clonal expansion in B cells in the periphery. Antibodies derived from these sequences have potent antibody binding capacity and support anti-

tumor immune responses. Whether similar tumor specific immune responses take place in the central nervous system needs to be determined.

Research goal

In this study we aimed to determine whether CSF B cells of patients with meningeosis neoplastica show signs of an immunogenic immune response and whether CSF B cells secrete antibodies into CSF and periphery. In a next step we analyzed whether the B cell response is tumor specific and identified potential targets of these B cells.

Materials and methods

Standard protocol approval and patients

The study was approved by the institutional review board of the University of Tübingen (972/2018B02 and 329/2019B01) and all patients gave written informed consent for their biological samples to be used for research purposes. Blood and CSF of 3 melanoma patients with meningeal carcinomatosis (see Table 4 for more details) and increased lymphocyte counts in the CSF (> 5 cells / µl) were acquired during routine clinical diagnostics. Serum and CSF supernatant were frozen at -80°C. Peripheral blood mononuclear cells (PBMCs) were extracted by Ficoll gradient (Histopaque, Sigma Aldrich) and frozen at -80°C until further processing. The MALME-3M melanoma cell line was purchased from the American Type Culture Collection (ATCC HTB-64) and primary fibroblasts of a healthy control subject (F-CO-49) were kindly provided by Prof. Schöls (Tübingen). The primary fibroblasts were derived from a skin sample of a 24 year old female healthy control.

Antibody extraction from CSF and serum

Samples were defrosted and briefly centrifuged to remove remaining debris. Pierce spin columns (Thermo Fischer Scientific) were used with Capture Select KappaXP Affinity Matrix (Thermo Fischer Scientific) and Capture Select LC-Lambda Affinity Matrix (Thermo Fischer Scientific). Serum was diluted 1:2 in PBS (Dulbecco's PBS, Sigma Aldrich), and CSF remained undiluted for processing according to the manufacturer's instructions. In brief, resin was washed with phosphate buffered saline (PBS, Dulbecco's PBS, Sigma Aldrich), incubated with sample for 10 minutes and again

washed with PBS. Antibodies were extracted by adding twice 100 µl of 0.1 M glycine solution (pH 2.5). Samples were transferred to the Core Facility for Medical Bioanalytics Tübingen for further processing and mass spectrometry.

Construction of patient specific B cell repertoires

The protocol was adapted from Owens and colleagues [107]. In short, for fluorescence assisted single cell sorting CSF cells were thawed in a 37 °C water bath and washed in PBS (Dulbecco's PBS, Sigma Aldrich). After centrifugation the cell pellet was resuspended in FACS Buffer (Dulbecco's (PBS, Sigma Aldrich), 2 % fetal calf serum (FCS, Thermo Fischer Scientific), 0.01 % NaN3 (Serva) and 2 mM EDTA (Merck). Cells were collected by centrifugation at 400 g for 4 minutes at 4°C. Subsequently, cells were suspended in FACS buffer and antibody mix was added. The antibody mix consisted of CD38(HB7) fluorescein isothiocyanate (FITC, Becton, Dickinson and Company, BD Biosciences), polyclonal rabbit anti-human IgD/RPE Phycoerythrin (PE, Dako, Agilent Technologies), CD19 Phycoerythrin-Texas Red-X (ECD, Beckman Coulter Company), CD20 (L27) Allophy-cocyanin-Cyanin7 (APC Cytm7, Becton, Dickinson and Company, BD Biosciences), CD3 (SK7) Phyco-erythrin-Cyanin 7 (PE Cytm7, Becton, Dickinson and Company, BD Biosciences), CD45 V450 mouse anti-human clone H130 (Becton, Dickinson and Company, BD Biosciences) and CD27 (L128) Allophycocyanin (APC, Becton, Dickinson and Company, BD Biosciences). After incubation for 30 minutes at 4°C in the dark, cells were washed twice with FACS buffer. Lastly, cells were resuspended in FACS buffer and filtered with a 40 µm nylon mesh. For compensation, beads (AbC Total Antibody compensation beads, Thermo) were stained with the antibodies according to the respective protocol. Single cell sorting of plasmablasts (CD45+ CD3- CD19+ CD20- CD27+ CD38++) was performed with the FACSAria III (BD). Lysis, cDNA synthesis and amplification protocols were adopted from Owens and colleagues [107]. PCR protocols were slightly adjusted and different primer sets were used. B cell heavy and light chains were sequenced by Eurofins Genomics (Germany). Sequences were copied into the Vbase2 database [108] and the amino acid sequence, CDR1-3 regions and V(D)J segments were retrieved. B cell sequences were grouped into clones when variable (VH) and joining (JH) segments of the heavy chain were identical (adopted from Kowarik and colleagues [109]). Mutations from germline were defined as divergence from the most probable VH segment suggested

by the Vbase2 database. Immunoglobulin variable heavy chain (IGHV) family distribution was determined by IMGT/VQuest [110] and plotted using Microsoft Excel 365 (Microsoft Corporation).

Library preparation for next generation sequencing

Library preparation of the entire B cell pool per patient was done as described previously [111]. In brief, lymphocytes were defrosted and bulk sorted using the flow cytometry panel described above (limited to CD45+, CD3-, and CD19+). RNA was extracted using the Nucleospin RNA Plus XS Kit (Machery Nagel) according to the manufacturer's instructions. Subsequently, Clontech SMARTer Ultra Low RNA Kit for Illumina sequencing (Takara Bio) was used to produce cDNA. cDNA was purified by AmpureXP beads (Beckman Coulter) and amplified using the expand high fidelity PCR System (Roche). Amplified DNA was again bead purified and subsequently gel extracted using the Nucelospin RNA Plus XS Kit (Machery Nagel). DNA was then quantified by qPCR (LightCycler® 480 SYBR Green Master, Roche) according to the manufacturer’s instructions. Finally, library was sequenced on an Illumina MiSeq Personal Sequencer with 250 bp paired-end sequencing by the Department of Microbiology in Tübingen. Repertoires were generated by the Quantitative Biology Center in Tübingen.

Overlap analyses

Overlap between blood and CSF B cell receptor sequences were determined using Python (Python Software Foundation, version 3.10, available at http://www.python.org). A match in the specific heavy chain V and J segments of two sequences from blood transcriptome and CSF transcriptome respectively was considered a clonal relationship.

Proteome and transcriptome overlap was also determined using Python. For general overlaps the peptide sequences derived from mass spectrometry were searched for in the CSF sequences determined by IMGT/V-QUEST [110]. To determine CDR overlaps complete CDRs of the single cell transcriptomes were searched in the peptide sequences derived from mass spectrometry in case they did not contain amino acids where digestion prior to mass spectrometry caused a cleavage (arginine (R) or lysine (K)) For CDRs from single cell transcriptomes which contained arginine or lysine only

strings larger than 3 amino acids up to or between arginine and/or lysine were used to map the sequence against the proteome.

Recombinant antibody production

We produced 7 recombinant antibodies for patient 1 which were derived from 6 clones. C7-P1 and H6-P1 originated from the largest clone and had light chains of different VH segments. 3 recombinant antibodies were produced for patient 2 and patient 3, respectively (see Table 4). For patient 2 these sequences were derived from different clones. For patient 3, two antibodies were produced from one clone each while E6-P3 originated from a sequence which could not be grouped. Recombinant antibodies were produced by Biointron (Zhangjiang, Shanghai).

Table 4 Patient characteristics and recombinant antibodies

Patient	Age	Treatment with checkpoint inhibitors	Antibody
1	69	no	H6-P1
			F6-P1
			B4-P1
			C4-P1
			B8-P1
			C7-P1
			H7-P1
2	29	yes	C2-P2
			C3-P2
			G4-P2
3	33	no	E1-P3
			F1-P3
			E6-P3

Table 4: Overview on patient characteristics and antibodies. We produced 7 antibodies for patient 1 and 3 antibodies each for patient two and three out of the different clones retrieved from single cell sequencing.

Flow cytometric assessment of antibodies

We tested whether our recombinant antibodies could bind a melanoma cell line Malme-3M or a non-neoplastic primary fibroblasts (F-CO-49). Cells were cultivated in Dulbecco's modified Eagle's Medium (DMEM, Sigma Aldrich) containing 10 % fetal bovine serum (Thermo Fischer) and 0.1 % Penicillin and Streptavidin (Sigma Aldrich). Cells were removed from the flask with trypsin (0.25 Trypsin EDTA, Sigma) and washed in PBS (Dulbecco's PBS, Sigma Aldrich). Subsequently, 100000 cells per sample were permeabilized with Cyto-Fast™ Fix/Perm Buffer Set (Biolegend) according to the manufacturer's instructions. Incubation with recombinant antibodies (25 µg per reaction) was followed by a wash step and the incubation with secondary PE anti-human IgG FC antibody (Biolegend). Finally, cells were washed, resuspended in FACS Buffer and measured on DAKO CyAnADP (Beckman Coulter) and analyzed using Summit V4.3 (Cytomation). To evaluate nonspecific binding, controls included secondary antibody only and primary antibody staining with normal human IgG control (Bio Techne).

Microarray

To screen for potential antigens on a larger scale the HuProt™ Human Proteome Microarray 4.0 was conducted by PEPperPRINT (Heidelberg). The 7 antibodies of the first patient as well as the 3 antibodies of the remaining two patients each were pooled and tested on the array. Analysis of the antibody pools was provided by PEPperPRINT.

ELISA

Recombinant proteins aldo-keto reductase family 1 member A1 (AKR1A1, LS Bio, phosphoribosylglycinamide formyltransferase (GART, Biotrend), magnesium dependent phosphatase 1 (MDP1, Biomol), peptidylprolyl isomerase like 1 (PPIL1, Hölzel), microtubule associated scaffold protein 2 (MTUS2, Bio Techne), DEAD-box helicase 53 (DDX53, MyBioSource), and aminoacylase 3 (ACY3, Hölzel) were dissolved in PBS (Dulbecco's PBS, Sigma Aldrich) and diluted to a final concentration of 100 ng/ ml. Coating was subsequently performed with 100 µl of each protein dilution on high binding plates (RnD) and incubated overnight. Three wash steps with 300 µl PBS containing 0.05 % Tween 20 (Serva) were followed by blocking in 300 µl 1 % albumin fraction

V (Roth) in PBS for 2 hours. After washing 100 µl of recombinant antibodies or IgG control (Bio techne) at a concentration of 5 µg/ ml in blocking buffer was added. As an additional negative control recombinant antibodies and control IgG were also incubated in uncoated wells not containing protein. After incubation of 2 hours, wells were washed again and 100 µl of biotinylated anti-human K light chain secondary antibody (Biolegend, dilution 1:2000 in blocking buffer) was added. Incubation for 1 hour was followed by another wash step. Subsequently, 100 µl HRP-streptavidin (Biolegend, 1:1000 diluted in blocking buffer) was incubated for 20 minutes. After a last wash, 100 µl tetramethyl benzidine (TMB) substrate (Biolegend) was incubated for another 20 minutes. 50 µl of stop solution (2N H_2SO_4 solution) was added and optical density was measured at a wavelength of 492 nm on the Sunrise Reader (TECAN, Crailsheim, Germany). Background noise (optical densities of the respective recombinant antibodies in uncoated wells) was subtracted from the experimental data. In some cases due to variations in measurement this resulted in very small negative values which were neglected and set to 0. Result figures were produced using Microsoft Excel 365 (Microsoft Corporation).

Results

Sequencing data

Single cell repertoires of the three patients were generated and consisted of 64 complete heavy and light chain pairs for patient 1, 30 complete heavy and light chain pairs for patient 2 and 9 complete heavy and light chain pairs for patient 3. B cell receptor sequences of only heavy or only light chains were additionally used to define clones. We identified 6 clones for patient 1, 5 clones for patient 2 and 3 clones for patient 3. The B cell repertoires further showed sequences with mutations from the most probable germline V segment in the framework regions as well as in the CDRs (Fig. 5).

We evaluated the distribution of IGVH family distribution and found differences between patients. Patient 1 had the largest abundance in IGVH4, while patient 2 showed mainly usage of IGHV1 and IGHV3. Patient 3 had a more balanced IGHV usage (Fig. 6). Differentiation between IgM and IgG plasmablast sequences could not be performed using IGMT/ VQuest [110].

Fluorescence assisted cell sorting in blood retrieved 70466 B cells for patient 1, 20052 B cells for patient 2 and 872989 B cells for patient 3. After sequencing, the resulting B cell repertoire was screened whether B cell receptors with the same V and J segments in the CSF could be found in the blood of each patient. There was no overlap in any of the patients' repertoires.

Transcriptome proteome mapping

It was determined whether peptide sequences from CSF and serum antibodies matched with the CSF B cell receptor repertoire. Matches were found in the framework regions as well as in the CDRs (Fig. 5).

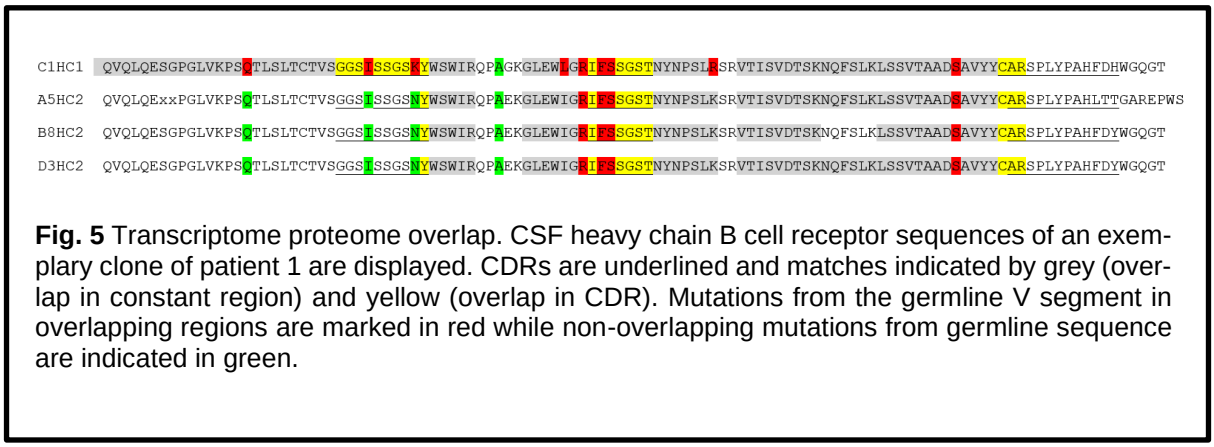

Fig. 5 Transcriptome proteome overlap. CSF heavy chain B cell receptor sequences of an exemplary clone of patient 1 are displayed. CDRs are underlined and matches indicated by grey (overlap in constant region) and yellow (overlap in CDR). Mutations from the germline V segment in overlapping regions are marked in red while non-overlapping mutations from germline sequence are indicated in green.

For overlap analyses only one of each unique CDR contained in complete sequences was analyzed. Overlap of CSF transcriptome and CSF proteome for patient 1 existed in 100 % of CDR1, 70 % of CDR2 and 44 % of CDR3. Serum proteins of patient one showed overlaps with CSF transcriptome in 69 % of CDR1, 50 % of CDR2 and 31 % of CDR3. The CDRs of the seven recombinant antibodies produced from this patient's repertoire could largely be found in the proteome (Table 5). For patient 2, overlaps between CSF transcriptome and CSF proteome could be found in 21 % of CDR1, 60 % of CDR2 and 14 % of CDR3. Serum protein and CSF transcriptome overlaps could be determined for 5 % of CDR1, 35 % of CDR2 and 14 % of CDR3. Patient 3 data produced overlaps in CSF transcriptome and CSF proteome of 20 % in CDR1, 50 % in CDR2 and 9 % in CDR3. Serum protein overlapped with the transcriptome in

20 % of CDR1, 30 % of CDR2 and 0 % of CDR3. Patient 2 and 3 CDR transcriptome sequences could hardly be found in the proteome (Table 5).

Flow Cytometry

Flow cytometry was conducted in a melanoma cell line Malme-3M and in primary fibroblasts of a healthy control subject. Cells were stained with the recombinant antibodies produced from the patient's CSF transcriptome. Staining patterns of these two cell lines appeared to be very similar (see Fig. 7 and 8). Although it is difficult to evaluate staining without positive controls, we considered recombinant antibodies H6-P1, F6-P1, B4-P1, B8-P1, C7-P1 and F1-P3 to be clearly positive while negative controls as well as recombinant antibodies C4-P1, E1-P3, E6-P3, C2-P2, C3-P2 and G4-P2 were considered negative. H7-P1 appeared to be slightly positive in Malme-3M cells and mostly negative in fibroblasts. Even though some of the cells stained with the antibodies considered negative had partially elevated intensities they could not be clearly differentiated from the negative controls.

Table 5 Overlap of recombinant antibody CDRs with CSF and serum proteome

Antibody	CDR1	CDR2	CDR3
H6-P1	CSF/Serum	CSF/Serum	CSF/Serum
F6-P1	CSF/Serum	CSF/Serum	CSF/Serum
B4-P1	CSF/Serum	CSF/Serum	-
C4-P1	CSF/Serum	CSF/Serum	-
B8-P1	CSF	CSF/Serum	-
C7-P1	CSF	CSF/Serum	CSF/Serum
H7-P1	CSF/Serum	-	-
C3-P2	-	-	-
C2-P2	-	CSF	-
G4-P2	-	CSF	-
E1-P3	-	-	-
F1-P3	-	CSF	-
E6-P3	-	-	-

Table 5: For the recombinant antibodies produced, overlaps of the CSF transcriptome CDRs with the proteome are evaluated. CSF indicates that overlaps were only found in the CSF proteins. CSF/Serum indicates that overlaps were found in both peripheral blood and CSF compartment.

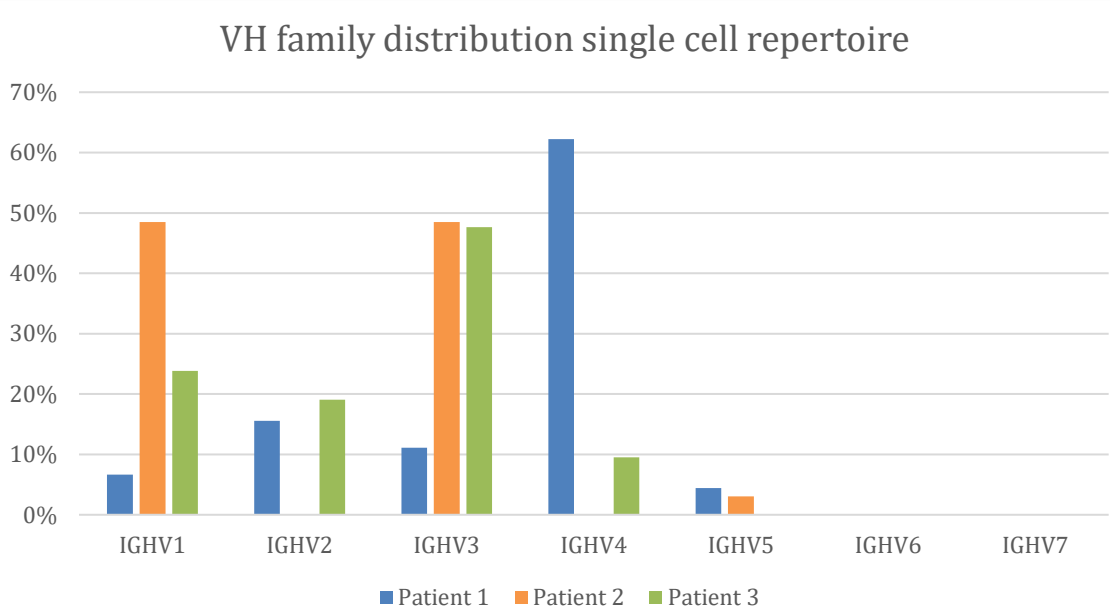

Fig. 6 VH family distribution in single cell repertoire. The distribution of the VH family usage in the single cell repertoire is presented. VH family usage was retrieved from IMGT/VQuest database.

Microarray

In a subsequent analysis we aimed to determine the target antigens of the recombinant antibodies by using a protein microarray. For the HuProt™ Human Proteome Microarray 4.0 a list of the first 50 antigen hits and corrected signals captured can be found in Table 6-7. Since there was a prominent cut-off after the first two proteins in the array batch of the last two patients, we considered these to be candidate target antigens for these antibodies. The cut-off for the antibody batch of patient 1 was not as obvious. However, within the first hits we identified 3 peptidylprolyl isomerases (PPIs) and two phosphatases. Further, 3 antigens were listed as either cancer enhanced or cancer enriched in the Human Protein Atlas [112,113]. We chose to further test one protein of each group (PPIs and phosphatases), namely peptidylprolyl isomerase like 1 (PPIL-1) and magnesium dependent phosphatase 1 (MDP1), and the three cancer associated antigens microtubule associated tumor suppressor candidate 2 (MTUS2), DEAD-box helicase 53 (DDX53) and aminocyclase 3 (ACY3) by ELISA to confirm target specificity of the individual recombinant antibodies.

ELISA

We measured optical densities (OD) of DDX53, AKR1A1, GART, PPIL-1, MDP-1, ACY-3 and MTUS2 for binding to the recombinant antibodies or control IgG (Fig. 9).

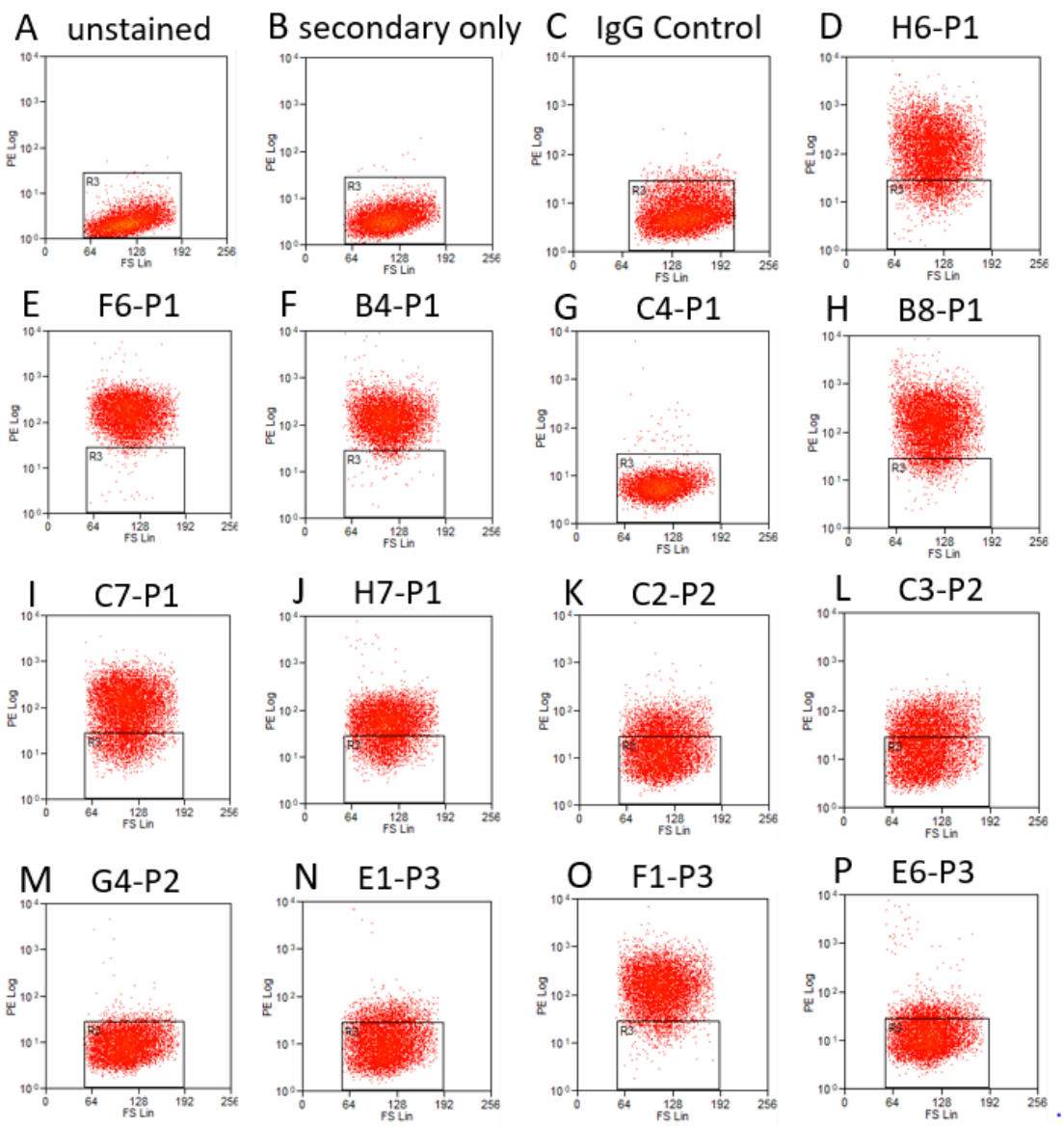

Fig. 7 Flow cytometry of recombinant antibodies in Malme3M cells. Malme 3M cells were stained as following: unstained, secondary antibody only, IgG Control, H6-P1, F6- P1, B4- P1, C4- P1, B8-P1, C7- P1, H7- P1, C2- P2, C3- P2, G4- P2, E1- P3, F1- P3, E6-P3. Gate R3 represents the location of the negative population.

Binding of control IgG to the proteins was very low (OD(range) = 0.02 - 0.06). Except from B8-P1 (OD = 0.52), F1-P3 (OD = 0.20) and F6-P1 (OD = 0.21) also binding of antibodies against uncoated wells was low. Anyway, to better understand specific binding of the antibodies, OD of background staining of the respective antibodies as determined by binding to uncoated wells was subtracted from test sample ODs.

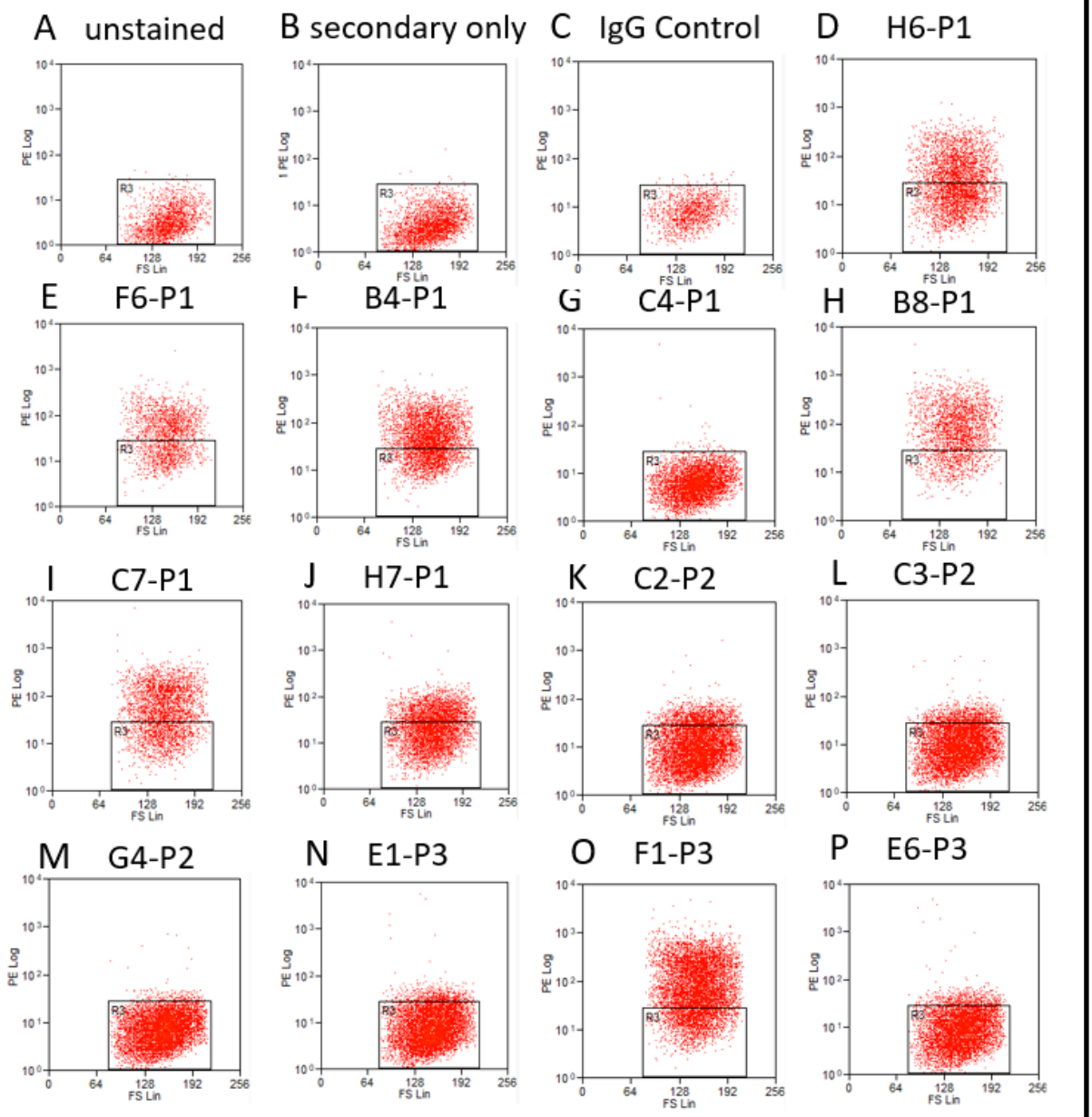

Fig. 8 Flow cytometry of recombinant antibodies in F-CO-49 cells: F-CO-49 cells were stained as following: unstained, secondary antibody only, IgG Control, H6-P1, F6- P1, B4- P1, C4- P1, B8-P1, C7- P1, H7- P1, C2- P2, C3- P2, G4- P2, E1- P3, F1- P3, E6-P3. Gate R3 represents the location of the negative population.

Subsequently, DDX53 had the strongest binding profile with B4-P1 (OD = 3.12) and H7-P1 (OD = 2.96) showing high binding (OD>2) to this protein. Additionally, F6-P1 (OD = 1.10), C4-P1 (OD = 1.79), E6-P3 (OD = 0.92) and C7-P1(OD = 0.57) showed moderate optical density values (OD>0.5). Generally, the other 6 proteins showed much weaker binding profiles. Binding of B8-P1 was superior in coated vs uncoated

Table 6 Microarray results patient 1

Name	UniProt ID	Full Name	Corrected Intensity Ratio
PPP1R12B	O60237-2	protein phosphatase 1 regulatory subunit 12B	1,309.2
PPIL1	Q9Y3C6	peptidylprolyl isomerase like 1	1,309.2
SHFM1	P60896	SEM1 26S proteasome complex subunit	1,309.1
RAD23A	P54725-3	RAD23 homolog A, nucleotide excision repair protein	1,309.1
LASP1	Q14847	LIM and SH3 protein 1	1,309.0
CCR1	P32246	C-C motif chemokine receptor 1	1,308.6
RAD23A	P54725	RAD23 homolog A, nucleotide excision repair protein	1,304.6
PPIE	Q9UNP9	peptidylprolyl isomerase E	1,297.1
NACA	Q13765	nascent polypeptide associated complex subunit alpha	1,295.7
SETD7	Q8WTS6	SET domain containing 7, histone lysine methyltransferase	1,288.3
APBB1	O00213	amyloid beta precursor protein binding family B member 1	1,287.9
ACBD3	Q9H3P7	acyl-CoA binding domain containing 3	1,269.5
WASF2	Q9Y6W5	WASP family member 2	1,206.0
PPIA	P62937	peptidylprolyl isomerase A	1,205.9
UBL7	Q96S82	ubiquitin like 7	1,203.9
GPBP1_frag		GC-rich promoter binding protein 1	1,175.1
NAPB	Q9H115	NSF attachment protein beta	1,172.1
DBNL	Q9UJU6	drebrin like	1,081.8
MTUS2	Q5JR59-3	microtubule associated scaffold protein 2	1,068.7
KCTD5	Q9NXV2	potassium channel tetramerization domain containing 5	1,051.5
LRRFIP1	Q32MZ4	LRR binding FLII interacting protein 1	1,048.3
SCL-70			1,007.5
CCDC102B_frag		coiled-coil domain containing 102B	984.8
KIFC3	Q9BVG8-5	kinesin family member C3	942.5
MDP1	Q86V88	magnesium dependent phosphatase 1	919.9
DBNL	Q9UJU6-2	drebrin like	918.3
PEX19	P40855	peroxisomal biogenesis factor 19	917.0
SF3A1	Q15459	splicing factor 3a subunit 1	914.2
CALCOCO2	Q13137	calcium binding and coiled-coil domain 2	899.4
LMNA		lamin A/C	894.4
SLC7A6OS	Q96CW6	solute carrier family 7 member 6 opposite strand	894.0
ACRC	Q96QF7	germ cell nuclear acidic peptidase	893.9
Hep B Protein X			865.0
DDX53	Q86TM3	DEAD-box helicase 53	864.5
ACY3	Q96HD9	aminoacylase 3	863.6
CRK	P46108	CRK proto-oncogene, adaptor protein	821.9
TEX13A	Q9BXU3	testis expressed 13A	819.2
PARVA	Q9NVD7	parvin alpha	816.2
PA2G4	Q9UQ80	proliferation-associated 2G4	776.7

CEP85	Q6P2H3-3	centrosomal protein 85	730.4
BRD2	P25440	bromodomain containing 2	706.4
NACA2	Q9H009	nascent polypeptide associated complex subunit alpha 2	701.7
PSMD7	P51665	proteasome 26S subunit, non-ATPase 7	683.1
GIPC1	O14908-2	GIPC PDZ domain containing family member 1	666.3
CABP4	P57796-2	calcium binding protein 4	651.7
KIFC3	Q9BVG8-5	kinesin family member C3	646.1
SMARCC1	Q92922	SWI/SNF related, matrix associated, actin dependent regulator of chromatin subfamily c member 1	592.2
PACSIN2	Q9UNF0	protein kinase C and casein kinase substrate in neurons 2	591.9
ASCC2	Q9H1I8	activating signal cointegrator 1 complex subunit 2	580.5
OTUD6B	Q8N6M0	OTU domain containing 6B	577.6

Table 6: The first 50 hits of the pooled 6 antibodies of patient 1 are displayed with their corrected intensity ratios provided by PEPperPRINT.

Table 7 Microarray results patients 2 and 3

Name	UniProt ID	Full Name	Corrected Intensity Ratio
AKR1A1	P14550	aldo-keto reductase family 1 member A1	1,309.3
GART	P22102-2	phosphoribosylglycinamide formyltransferase, phosphoribosylglycinamide synthetase, phosphoribosylaminoimidazole synthetase	1,308.9
RHOA	P61586	ras homolog family member A	786.9
SHFM1	P60896	SEM1 26S proteasome complex subunit	718.2
RAC3	P60763	Rac family small GTPase 3	715.4
RAB11A	P62491	RAB11A, member RAS oncogene family	709.4
SNX9	Q9Y5X1	sorting nexin 9	638.4
OFD1_frag		OFD1 centriole and centriolar satellite protein	606.5
NAPB	Q9H115	NSF attachment protein beta	582.7
SLC7A6OS	Q96CW6	solute carrier family 7 member 6 opposite strand	548.9
OFD1_frag		OFD1 centriole and centriolar satellite protein	519.2
RAP1GDS1	P52306-2	Rap1 GTPase-GDP dissociation stimulator 1	506.6
ING3	Q9NXR8-2	inhibitor of growth family member 3	471.9
PMEPA1	Q969W9-2	prostate transmembrane protein, androgen induced 1	442.0
XRCC4	Q13426	X-ray repair cross complementing 4	440.7
CCDC102B_frag		coiled-coil domain containing 102B	438.4
ACSL4	O60488-2	acyl-CoA synthetase long chain family member 4	403.1
ARFGAP1	Q8N6T3-2	ADP ribosylation factor GTPase activating protein 1	377.3
MED22	Q15528-2	mediator complex subunit 22	362.8
USP5	P45974	ubiquitin specific peptidase 5	360.9
PPM1B	O75688-2	protein phosphatase, Mg2+/Mn2+ dependent 1B	348.5
RAC1	P63000	Rac family small GTPase 1	323.9

PPM1J	Q5JR12	protein phosphatase, Mg2+/Mn2+ dependent 1J	312.9
NAP1L1	P55209	nucleosome assembly protein 1 like 1	312.6
XRCC4	Q13426-3	X-ray repair cross complementing 4	292.5
ZFYVE16	Q7Z3T8-3	zinc finger FYVE-type containing 16	289.2
TLE3	Q04726	TLE family member 3, transcriptional corepressor	283.5
PPM1D	O15297-2	protein phosphatase, Mg2+/Mn2+ dependent 1D	272.7
ARFGAP1	Q8N6T3	ADP ribosylation factor GTPase activating protein 1	272.6
APBB1	O00213	amyloid beta precursor protein binding family B member 1	269.8
ARHGEF16	Q5VV41-2	Rho guanine nucleotide exchange factor 16	268.6
PDCL	Q13371	phosducin like	267.9
TSEN15	Q8WW01	tRNA splicing endonuclease subunit 15	241.3
SCYL3	Q8IZE3-2	SCY1 like pseudokinase 3	236.9
RBBP7	Q16576	RB binding protein 7, chromatin remodeling factor	235.5
CSNK1G1	Q9HCP0-2	casein kinase 1 gamma 1	221.6
PVRL3_frag		nectin cell adhesion molecule 3	210.7
C14orf37	Q86TY3	armadillo like helical domain containing 4	210.2
RAB2B	Q8WUD1	RAB2B, member RAS oncogene family	208.8
EEF2K	O00418	eukaryotic elongation factor 2 kinase	208.7
BRD2	P25440	bromodomain containing 2	706.4
NACA2	Q9H009	nascent polypeptide associated complex subunit alpha 2	701.7
PSMD7	P51665	proteasome 26S subunit, non-ATPase 7	683.1
GIPC1	O14908-2	GIPC PDZ domain containing family member 1	666.3
CABP4	P57796-2	calcium binding protein 4	651.7
KIFC3	Q9BVG8-5	kinesin family member C3	646.1
SMARCC1	Q92922	SWI/SNF related, matrix associated, actin dependent regulator of chromatin subfamily c member 1	592.2
PACSIN2	Q9UNF0	protein kinase C and casein kinase substrate in neurons 2	591.9
ASCC2	Q9H1I8	activating signal cointegrator 1 complex subunit 2	580.5
OTUD6B	Q8N6M0	OTU domain containing 6B	577.6

Table 7: The first 50 hits of the pooled 7 antibodies of patients 2 and 3 are displayed with their corrected intensity ratios provided by PEPperPRINT.

wells for AKR1A1 (OD = 0.20), MTUS2 (OD = 1.61) and ACY-3 (OD = 0.46). F1-P3 showed higher ODs for AKR1A1 (OD = 0.41), and MTUS2 (OD = 0.21) and F6-P1 showed increased ODs for MTUS2 (OD = 0.24) when compared to uncoated wells and control IgG but binding was still very weak. The remaining antibodies did not show relevant binding patterns (OD<0.2).

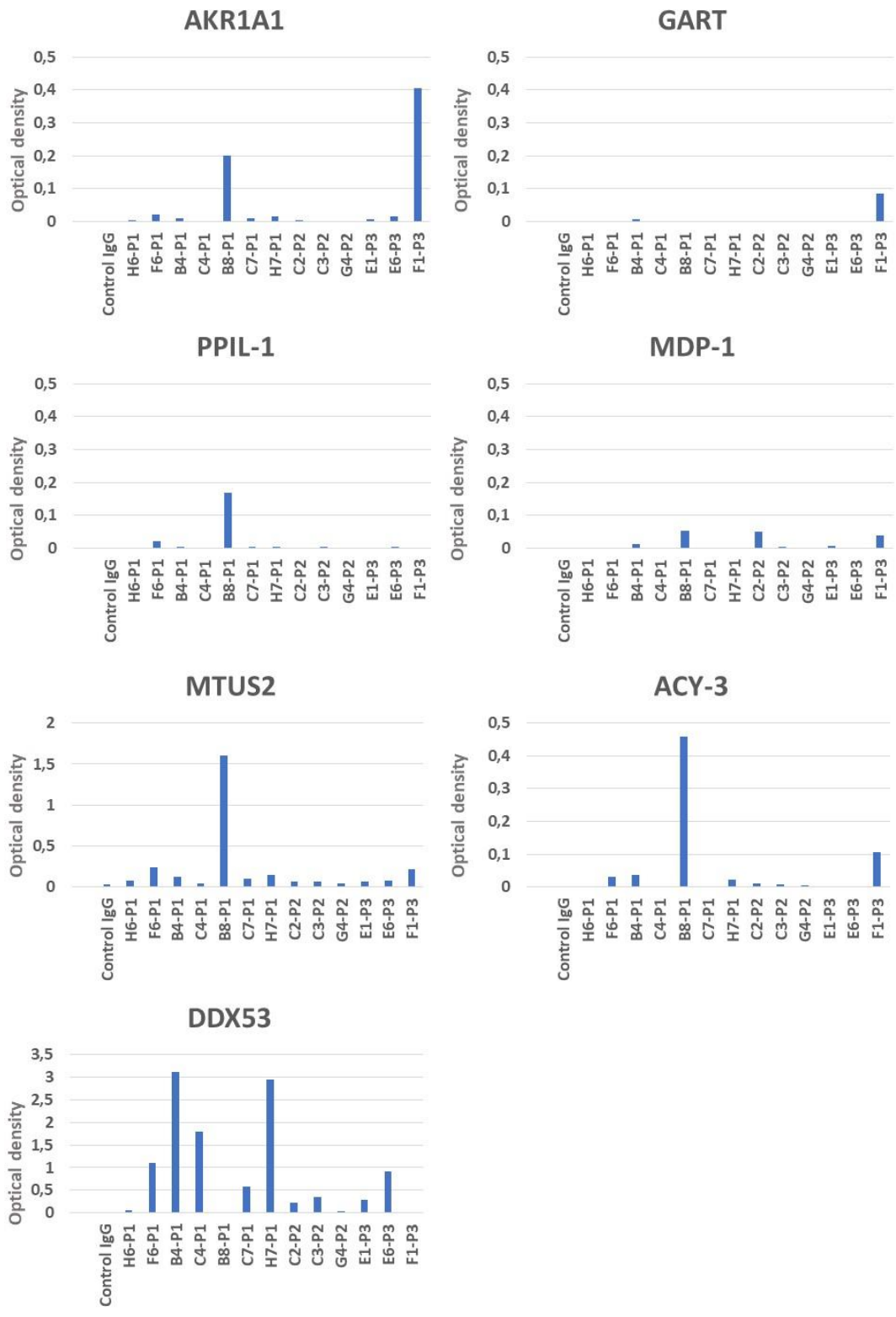

Fig. 9 ELISA for selected proteins**.** Enzyme linked immunosorbent assay was conducted for proteins AKR1A1, GART, PPIL1, MDP1, ACY3 and MTUS2 using IgG Control, H6-P1, F6- P1, B4-P1, C4- P1, B8-P1, C7- P1, H7- P1, C2- P2, C3- P2, G4- P2, E1- P3, F1- P3 and E6-P3. Reactivity of antibodies against the uncoated wells were subtracted. Values on the Y axis are optical densities determined experimentally.

Discussion

In this project we analyzed CSF B cells of patients with metastatic spread of melanoma cells to the brain in order to evaluate whether a specific B cell response occurs within the CNS compartment. CSF B cells were clonally expanded and overlapped with the immunoglobulin peptides from CSF and serum indicating that CSF B cells indeed produce and secrete antibodies in the CSF compartment. Recombinant antibodies produced from these clones showed similar binding patterns in non-neoplastic primary fibroblasts and in a malignant melanoma cell line indicating that potential targets might be expressed on tumor tissues as well as other cell types. Additionally, some proteins could be identified as potential targets by protein microarrays.

Transcriptomic and proteomic analysis

B cell repertoire sequencing of 3 meningeosis neoplastica patients on single cell level revealed expanded B cell clones. These clones showed mutations from germline not only in the framework regions but also in the CDRs. This suggests that these cells have had antigen contact and have subsequently undergone affinity maturation processes with mutations in binding relevant regions [114]. Since these patients not knowingly suffered from another neurological disease this strongly supports the hypothesis that B cells arising in the CSF of these patients are related to an immune response most likely triggered by the invading tumor cells.

To further evaluate the relevance of these B cells we overlapped the sequences retrieved from single cell sequencing with the amino acid sequences from mass spectrometry. While the B cell receptor sequences are derived from B cell transcriptomes, mass spectrometry offers the possibility to characterize antibodies directly in serum and CSF. The assumption is that a sequence match between the compartments indicates that this antibody was produced by a clone of the respective B cell with the same receptor sequence [109]. Evidence is especially strong when the matching sequences contain somatic mutations in the CDRs since a specific CDR3 region can be regarded as a fingerprint of the respective B cell clone [92]. Indeed, mass spectrometry derived peptides from serum and CSF matched with amino acid stretches from B cell receptors retrieved from CSF single cell sequencing in both constant regions and CDRs (Fig. 5). It is thus very likely that these CSF B cell clones produce antibodies which circulate in the CSF and the periphery.

To determine whether similar B cell clones reside in the peripheral blood which could have produced these antibodies we next sequenced the blood repertoire of these 3 patients by NGS. Since the melanomas originated in the periphery and only metastasized later to the CNS it seems likely that tumor targeting antibodies are also present in the blood compartment. However, no clonal relatives of the CSF B cells could be found in the blood. This could be due to the relatively small repertoire which can be produced from CSF B cells. The smaller the repertoire, the less likely is a match with the naturally large peripheral blood B cell repertoire. We thus cannot exclude that progenitor B cells exist in the periphery which gave rise to the B cell population in the CNS. The current data however indicates that the B cell response is rather localized to the central nervous system.

Alternatively, the lack of transcriptome overlap between blood and CSF compartment may be explained by a change in tumor antigen expression. It has been shown that the antigen expression in melanoma changes over the disease course and metastases may have different antigen phenotypes compared to the primary tumors [115]. This may have also influenced the CSF B cell repertoire to diverge from the peripheral B cell repertoire.

Target characterization and specificity

As a next step we tried to determine the antigen targets of these CSF B cells. We produced recombinant antibodies and tested these against a melanoma cell line and primary fibroblasts of a healthy control subject. Interestingly, the binding patterns of both cell lines show great similarity. Some antibodies (C4-P1, E1-P3, E6-P3, C2-P2, C3-P2 and G4-P2) were considered negative in both cell lines and may either bind an antigen not present on this specific melanoma cell line (e.g. neoantigens) or may not have strong binding capacity in general. On the other hand, some antibodies (H6-P1, F6-P1, B4-P1, B8-P1, C7-P1 and F1-P3) showed positive staining in both cell lines. This is astonishing since the primary fibroblasts were derived from healthy cells and should not express tumor antigens. One possible explanation is that these antibodies target “normal” intracellular proteins. This could be due to tumor cell death in the CNS, e.g. due to the shear pressure in the CSF [116], which exposes cell debris to the immune system. In case of sufficient antigenicity of the protein itself and adjuvant signals

in the form of danger associated molecular patterns the immune response can be initiated [117]. Generally, antigenicity of regular proteins should be low since B cells targeting healthy tissues would normally be negatively selected or put into a state of anergy [118]. However, we cannot exclude that this mechanism was surpassed by the cancer treatment. For example, checkpoint inhibitors interfere with the tolerance mechanisms of the immune system and could have supported the development of these self-reactive antibodies. Interestingly, however, antibodies of patient 2 - who to our knowledge received checkpoint inhibitors - did not present with relevant binding to the cell line.

Alternatively, at least some of the recombinant antibodies are not specific and show cross reactivity to other proteins which may be mistaken for the true targets. This is in line with the microarray results where the antibody batches show reactivity to a large amount of proteins at a similar level. It is in general possible that the antibodies bind antigens not included in these microarrays since mutated proteins are not captured in these assays. However, to determine neoantigens with recombinant antibodies showing strong cross reactivity with other proteins is challenging. In an attempt to characterize the antibody binding site a peptide library was used as described previously [119]. The library consisted of phage displaying about 10^9 unique peptides (Ph.D.-12™ Phage Display Peptide Library, New England Biolabs). They were exposed to a recombinant antibody with the sequence of C4 showing reactivity to DDX53 in a preliminary analysis with the Lung Cancer IgG Autoantibody Array (Ray Biotech). Antibody bound phage were amplified and introduced to the same antibody in the next round of panning. The assumption is that during 3 rounds of panning amino acid sequences with the highest affinity to the antibody would be selected. However, after sequencing phage and comparing the amino acid sequences no consensus sequence could be identified. Moreover, the antibody conformation was predicted using SAbPred [120] which was then applied to predict the respective epitope on the DDX53 protein using EpiPred [121]. The most likely amino acid stretches of the epitope were compared to the sequences displayed by the retrieved phage. Nevertheless, no clear overlaps could be found. It is possible that the experimental design still needs to be optimized to determine the antigens. Alternatively, these antibodies may not have a very specific target, but rather react to a variety of epitopes.

Another way to approach the understanding of antibody specificity is by taking a closer look at the CDRs of the recombinant antibodies. The CDRs in antibodies are generally considered the most important amino acid stretches for antigen binding among which the CDR3 region is especially variable in sequence and length [122]. Affinity maturation processes including changes in sequence due to somatic hypermutations can lead to a rigidification of the CDR3 loop [123]. This decreased flexibility of the paratope has been proposed to aid in reducing cross reactivity with other proteins [124]. Moreover, CDR3 regions can also be elongated by using more distant J and V gene segments in secondary gene rearrangement or by the introduction of insertions during germinal center reactions [125]. There is some evidence that CDR3 length has strong – if not – even superior influences on antibody specificity than the exact sequence [126].

To date it is unclear whether a longer CDR3 length is indicative of an antibody advantage - such as neutralizing capacity in broadly neutralizing anti-HIV antibodies [125]. In a comparative analysis between acute infections, chronic viral infections and systemic autoimmune disease Breden and colleagues [125] analyzed CDR3 length and level of somatic mutation. They found that chronic infections were associated with relatively long CDR3s while acute infections showed relatively short CDR3s. Autoimmune disease showed medium CDR3 lengths. Additionally, chronic viral infections were associated with high levels of somatic mutations and usage of more distal gene segments. This evidence is in line with the hypothesis of increasing antibody specificity by CDR3 somatic mutation and CDR3 elongation. On the contrary, Collis and colleagues [127] could find significant correlations between CDR3 length and antigen classes indicating that CDR3 length could also be a function of specific target characteristics. This is supported by evidence that a subset of melanoma derived antibodies showed even shorter CDR3s than circulating B cells [114]. The CDR3s of the recombinant antibodies produced in the study presented in this dissertation varied between 12-17 amino acids for patient 1, 8-18 amino acids for patient 2 and 11-22 amino acids for patient 3 while an average CDR3 length of 14.76 amino acids has been reported in healthy controls [128]. As a comparison, CDR3 length in broadly neutralizing antibodies in HIV were on average 20.9 amino acids long [125]. In summary, the relatively normal CDR3 lengths of the recombinant antibodies produced in this study could therefore be due to specific target characteristics as well as a relatively short exposure to central nervous system immunity as in acute compared to chronic infections.

Nevertheless, characterization of antibody targets based on sequence similarity is still challenging. Different antigenic structures require specific contacts with antibodies [129]. These interactions are not necessarily limited to individual CDRs or chains, thus more advanced methods than heavy chain CDR3 sequence similarity to characterize antibody targets are needed [129].

Promising target DDX53

Among the target proteins tested by ELISA, DDX53 (DEAD Box helicase 53, CAGE) had the strongest binding profile with the recombinant antibodies. Additionally, DDX53 was among the top 50 protein hits in the protein microarray and showed positive staining in the RayBiotech lung cancer array. It is part of the group of cancer testis antigens which are normally limited to germ cells, but are expressed in a variety of tumor types most likely due to transcriptional regulation by hypomethylation of the respective genes [130]. Cancer testis genes have been proposed to promote tumorigenesis by regulating oncogenic pathways involved in proliferation, angiogenesis, immortality, growth inhibition, apoptosis, genome integrity and metabolism [130]. DDX53 in particular has been associated with dysregulation in angiogenesis, autophagy and cancer stemness properties [130–132]. This protein can be identified as malignant by the immune system as indicated by the presence of autoantibodies in gastric cancer patients [133] and may therefore be a suitable target for immunotherapy.

Alternative target MTUS2

MTUS2 showed the second highest binding to recombinant antibody B8-P1. According to the Human Protein Atlas MTUS2 is considered a cancer enhanced protein [112]. It has further been identified to be among the top 10 driver oncogenes in breast cancer [134]. However, little is still known about MTUS2 in tumors and further research needs to identify its potential for therapeutic applications.

Evaluation of target specificity

Recombinant antibody B4-P1 showed strong binding to DDX53 in the RayBiotech lung cancer protein array as well as in the ELISA assay. Additionally, different clones of patient 1 showed at least moderate binding to DDX53 in ELISA. Likewise, B8-P1 showed substantially higher optical densities against MTUS2 compared to the remain-

ing recombinant antibodies suggesting DDX53 and MTUS2 as a likely target for a tumor induced immune response in patient 1. On the contrary, both proteins were not among the top hits in the HuProt microarray. It can be speculated that B cell maturation was still at stages too early for the production of highly specific antibodies. Further research is thus necessary to determine the specificity of the recombinant antibodies against DDX53 and MTUS2.

Limitations

Transcriptome and proteome

We analyzed the B cell receptor repertoire in CSF and blood and the respective proteome of three mengingeosis neoplastica patients. For patient 1, blood and CSF sampling happened a few weeks apart due to clinical routine schedules, but this is not expected to have a strong influence on the repertoire. The blood samples for NGS before and after lumbar puncture were thus combined to profit from larger cell counts and more reliable data. Sampling of CSF was overall limited as only left over CSF from clinical routine diagnostics was used.

Flow cytometry

A flow cytometric analysis was done to test whether the recombinant antibodies differ in binding between a normal and a non-neoplastic primary fibroblasts. Since the aim of this project was to determine the targets of theses recombinant antibodies there were no positive controls. It was therefore decided that a large amount of antibody (25 µg) was used to produce visible effects. The drawback of this method is that unspecific binding can bias the results. This is why we accepted slightly shifted populations and only considered populations with strong fluorescence shifts as truly positive. Subsequently we found 6 antibodies to be clearly positive.

Another difficulty in measuring recombinant antibody binding to the cell line is the fluorescent labeling. It was determined that using fluorescent secondary antibodies was the most reliable method of visualizing binding. The populations appear to be slightly spread out, possibly because not all recombinant antibodies may be bound by the same amount of secondary antibody. Alternatively, our targets may also be differently

expressed in single cells during a cell cycle and can therefore have various intensities in flow cytometry.

Microarray and ELISA

We conducted a microarray to screen for potential antigens and subsequently tried to verify these targets by ELISA. Concerning these tests some points need to be raised.

Firstly, since the microarray was measured in batches (all antibodies of patient 1 combined and patient 2 and 3 combined) it is not clear which antibodies were responsible to which degree for the hit list. Interestingly, MDP-1, identified by the microarray, did not show relevant binding in the ELISA. In contrast to the recombinant MDP-1 protein in the microarray which was produced by yeast the ELISA protein was produced in Escherichia Coli (E. Coli). However, MDP-1 does not have glycosylation sites as predicted by NetNGlyc - 1.0 [135] that could have been affected by the production in different species. Nevertheless, the MDP-1 recombinant protein used for ELISA also has only partly overlapping sequences with the MDP-1 microarray protein (see Table 7). It is possible that antibody binding in the protein microarray occurred in these non-overlapping regions and could therefore not be replicated in ELISA. PPIL-1, MTUS2, DDX53 and ACY-3 results also could have been biased by different glycosylation (see Table 7). This may also explain why DDX53 has the strongest binding pattern among the proteins tested in ELISA while being only the 34th ranked protein in the microarray.

Secondly, normal human IgG was used as negative control. This mixture of IgG consists of lambda and kappa light chains. Since the secondary antibody in ELISA was directed against the kappa chain, the optical density may have been underestimated. However, the ratio of kappa : lambda light chains is approximately 2:1 [136] and therefore even an increase of one third in signal would still be very low and an appropriate negative control.

Thirdly, F1-P3, F6-P1 and B8-P1 show increased optical densities even in uncoated wells. Blocking was performed with 1 % BSA in PBS and normal human IgG control showed very low optical densities in uncoated wells. These increased optical densities of F1-P3, F6-P1 and B8-P1 may be explained by a reactivity against BSA or an increased reactivity of the paratope in general. However, since these antibodies are also

among the ones showing positive staining in FACS they are likely the main contributors to the microarray results and target binding and may be particularly important.

Outlook to further studies

Lastly, a preliminary approach was taken to determine patient specificity of the recombinant antibodies by targeting resected tumor material of patient 1. This in turn would support the hypothesis of a targeted immunological response of B cells in the CSF against the tumor in patients with metastatic brain disease. The major difficulty in this approach is the use of human antibodies to target human material, since the secondary antibody used for detection may also bind endogenous antibodies in the tissue causing high background noise [137]. Some methods have been proposed to overcome these issues including direct detection or pre-labelling of the human antibody before introducing it to the tissue [137,138]. An additional problem is – as in the previous experiments – that the precise target is not known. Since it is unclear which proteins are targeted by the antibodies it is difficult to choose appropriate positive and negative controls. Especially in the light of the data described above the antibodies may have strong cross reactivity or may even target “normal” proteins which are present in the majority of human cells. It thus requires a sophisticated protocol.

Therapeutic applications

Even though these studies comprise basic research a perspective on possible therapeutic applications shall be presented.

Firstly, the discovery of tumor specific antibodies could directly be translated to the clinics. Native antibodies can target extracellular proteins and induce antibody dependent cell- or complement mediated cytotoxicity in the tumor [139]. The application of monoclonal antibodies in cancer therapy has gained increasing attention with clinical success in various cancer types, but suitability of the antigen is crucial [139]. Many tumor associated or oncogenic proteins are nucleus localized or cytoplasmatic and can therefore not be directly detected by antibodies [139]. However, these tumor antigens can be exposed to antibodies by necrosis of tumor cells or MHC class I presentation leading to an immunological response [139]. Since the role of auto-antibodies

can be double edged – tumor supportive as well as tumor destructive – [100] the applicability of autoantibodies in tumor therapy needs to be ultimately determined in preclinical and clinical trials.

Additionally, tumor specific antibodies can be used for the localized application of cytotoxic drugs improving their effectiveness [140]. These conjugates require a highly specific antibody against a tumor surface antigen, a stable linker which releases the payload at the right moment while keeping it in a non-toxic state during delivery and an extremely potent cytotoxic drug [140].

Secondly, not the antibodies themselves but the antibody producing B cell may be used for immunotherapy [141]. Moutai and colleagues [142] induced plasma cells from specificity selected germinal center like mouse B cells which after autologous transfer continued to produce target specific antibodies for several weeks. Moreover, B cells offer further advantages such as their ability to present antigen, homing to lymph nodes and long term persistence [141]. Nonetheless, it is questionable - especially when looking for B cells producing the determined recombinant antibodies – whether sufficiently large amounts of B cells can be retrieved.

Lastly, using recombinant antibodies of CSF B cells may help to identify relevant tumor targets. They most likely are capable of inducing an immune response since they already triggered the clonal expansion of B cells and the production of functional antibodies. Due to their accessibility, surface molecules are easier targets for antibodies [139]. However, it may also be possible to use intracellular tumor associated or tumor specific antigens, which can be translated into a therapeutic T cell driving vaccine. While TAA antigens often suffer from being expressed in a variety of tissues and exerting immunological tolerance, TSAs are very specific for the tumor, but cannot be applied to a large group of patients due to antigen heterogeneity [143]. The suitability of individual targets thus needs to be tested. Nevertheless, vaccines have gained much interest due to their potential to induce long lasting responses and immune memory offering promising advancements for the future [143].

Table 7 Sequence differences between protein microarray and ELISA

Name	Host species	Number of gly-cosylation sites	Sequence
AKR1A1	E.Coli	0	MAARVLIIGSGGREHTLAWKLAQSHHVKQVLVAPGNAGTACSEKISNTAISISDH- TALAQFCKEKKIEFVVVGPEAPLAAGIVGNLRSAGVQCFGPTAEAAQLESSKRFAKEFMDRHGIPTAQWKAFTKPEEACSFILSADFPALVVKASGLAAGKGVIVAKS KEEACKAVQEIMQEKAFGAAGETIVIEELLDGEEVSCLCFTDGKTVAPMPPAQDHKRLLEGD- GGPNTGGMGAYCPAPQVSNDLLLKIKDTVLQRTVDGMQQEGTPYTGILYAGIMLTKNGPKVLEFNCRFGDPECQVILPLLKSDLYEVIQSTLDGLLCTSLPVWLENH TALTVVMASKGYPGDYTKGVEITGFPEAQALGLEVFHAGTALKNGKVVTHGGRVLAVTAIRENLISALEEAKKGLAAIKFEGAIYRKDVGFRAIAFLQQPR
GART	Wheat	0	MAASCVLLHTGQKMPLIGLGTWKSEPGQVKAAVKYALS- VGYRHIDCAAIYGNEPEIGEALKEDVGPGKAVPREELFVTSKLWNTKHHPEDVEPALRKTLADLQLEYLDLYLMHWPYAFERGDNPFPKNADGTICYDSTHYKETWK ALEALVAKGLVQALGLSNFNSRQIDDILSVASVRPAVLQVECHPYLAQNELIAHCQARG- LEVTAYSPLGSSDRAWRDPDEPVLLEEPVVLALAEKYGRSPAQILLRWQVQRKVICIPKSITPSRILQNIKVFDFTFSPEEMKQLNALNKNWRYIVPMLTVDGKRVPR DAGHPLYPFNDPY
PPIL1	E.Coli	2	MAAIPPDSWQPPNVYLETSMGIIVLELYWKHAPKTCKNFAELARRGYYNGTKFHRIIKDF- MIQGGDPTGTGRGGASIYGKQFEDELHPDLKFTGAGILAMANAGPDTNGSQFFVTLAPTQWLDGKHTIFGRVCQGIGMVNRVGMVETNSQ DRPVDDVKIIKAYPSG
MDP1	E.Coli	0	MGSSHHHHHHSSGLVPRGSHMGSHMARLPKLAVFDLDYTLWPFWVDTHVDPPFHKS- SDGTVRDRRGQDVRLYPEVPEVLKRLQSLGVPGAAASRTSEIEGANQLLELFDLFRYFVHREIYPGSKITHFERLQQKTGIPFSQMIFFDDERRNIVDVSKLGVTCIHI QNGMNLQTLSQGLETFAKAQTGPLRSSLEESPFEA
MTUS2	Wheat	2	MGHCCCKPYNCLQCLDKTNESALVKEKELSIELANIRDEVAFHTAKCEKLQKEKEELERRFE- DEVKRLGWQQQAELQELEERLQLQFEAEMARLQEEHGDQLLSIRCQHQEQVEDLTASHDAALLEMENNHTVAITILQDDHDHKVQELMSTHELEKKELEENFEKLR LSLQDQVDTLTFQSQSLRDRARRFEEALRKNTEEQLEIALAPYQHLEEDMKSLKQVLEM- KNQQIHEQEKKILELEKLAEKNIILEEKIQVLQQQNEDLKARIDQNTVVTRQLSEENANLQEYVEKETQEKKRLSRTNEELLWKLQTGDPTSPIKLSPTSPVYRGSSSG PSSPARVSTTPR
DDX53	E.Coli	1	MSHWAPEWKRAEANPRDLGASWDVRGSRGSGWSGPFGHQGPRAAGSREPPLCFKIKNNMVGV- VIGYSGSKIKDLQHSTNTKIQIINGESEAKVRIFGNREMKAKAKAAIETLIRKQESYNSESSVDNAASQTPIGRNLGRNDIVGEAEPLSNWDRIRAAVVECEKRKWADL PPVKKNFYIESKATSCMSEMQVINWRKENFNITCDDLKSGEKRLIPKPT- CRFKDAFQQYPDLLKSIIRVGIVKPTPIQSQAWPIILQGIDLIVVAQTGTGKTLSYLMPGFIHLDSQPISREQRNGPGMLVLTPTRELALHVEAECSKYSYKGLKSICIYG GRNRNGQIEDISKGVDIIIATPGRLNDLQMNNSVNLRSITYLVIDEADKMLDMEFEPQIR- KILLDVRPDRQTVMTSATWPDTVRQLALSYLKDPMIVYVGNLNLVAVNTVKQNIIVTTEKEKRALTQEFVENMSPNDKVIMFVSQKHIADDLSSDFNIQGISAESLHGN SEQSDQERAVEDFKSGNIKILITTDIVSRGLDLNDVTHVYNYDFPRNIDVYVHRVGYIGRT- GKTGTSVTLITQRDSKMAGELIKILDRANQSVPEDLVVMAEQYKLNQQKRHRETRSRKPGQRRKEFYFLS
ACY3	E.Coli	2	MGSSHHHHHHSSGLVPRGSHMGSMCSLPVPREPLRRVAVTGGTHGNEMS- GVYLARHWLHAPAELQRASFSAVPVLANPAATSGCRRYVDHDLNRTFTSSFLNSRPTPDDPYEVTRARELNQLLGPKASGQAFDFVLDLHNTTANMGTCLIAKSSH EVFAMHLCRHLQLQYPELSCQVFLYQRSGEESYNLDSVAKNGLGLELGPQPQGVLRA- DIFSRMRTLVATVLDFIELFNQGTAFPAFEMEAYRPVGVVDFPRTEAGHLAGTVHPQLQDRDFQPLQPGAPIFQMFSGEDLLYEGESTVYPVFINEAAYYEKGVAFV QTEKFTFTVPAMPALTPAPSPAS

Table 7: recombinant protein characteristics for ELISA are displayed. Host species is either Escherichia coli (E.Coli) or wheat. The highlighted sequence marks the sequence overlap between ELISA and microarray.

Evaluation

The second study suggests that B cells in the CSF of patients with metastatic melanoma are a result of an immunological reaction against the tumor. This makes these B cells valuable tools for further investigations on anti-tumor immune responses and target detection. However, it still needs to be determined whether the CSF immune response is specific enough to translate these findings into clinical applications.

Overall summary and conclusions

The role of B cells in cancer has long not been adequately considered to understand immunological mechanisms. We therefore evaluated the role of B cells in two tumor entities.

We could not find a large infiltration of lymphocytes – and thus also B cells - in glioma tissues. Accordingly, we assume that they do not play a major role in glioma associated immune responses. In glioma, macrophages seem to be the major players in the tumor microenvironment and interact with the cytokine milieu. It is therefore reasonable to target these cells in immunotherapeutic approaches. Since cytokines were correlated with macrophages, attempts should be made to determine cytokine patterns as biomarkers for better disease assessment and more personalized therapies.

In contrast, we have shown that in metastatic melanoma B cells can trigger immune responses which may be exploited for the development of new immunotherapies. Antigens derived from B cells may be promising targets since they have shown to successfully induce immune response potentially even overcoming tolerance mechanisms and autoreactivity. CSF B cell targets in specific also do not have to be disentangled from everyday life pathogen triggered immune responses. In the light of the large health burden still associated with cancer it is urgently necessary to discover new targets for successful immunotherapy.

Since we have argued in the first part of this work that the CSF may be considered a part of the immunological microenvironment it is reasonable to study also the antibody mediated immune response of B cells in this region. Due to its immunogenic properties metastatic melanoma was a more suitable model for this [77]. We could

show that B cell maturation and antibody production take place in the CSF. This strongly supports the role of the CSF as a surrogate marker for immune activation for different cell types as well as tumor entities.

Even though tumor entities may differ in the way they activate the immune system, results from different tumor types may aid to get a more general understanding of tumor immunology. Immune target detection in immunologically hot tumors may help to identify immunotherapy targets in immunologically cold tumors. Nonetheless, it remains speculative to this point whether different tumor entities share a common immunological structure.

To date, immunotherapy can be considered the most promising approach to treating tumors. Filling the knowledge gap and understanding how the immune system truly responds to cancer has the potential to revolutionize efficacy, overall survival and treatment related side effects.

Statement of contributions

Study 1

In this study I was involved in the application for ethical approval, the process of developing the experimental design, the application for the biological material, the measurement of the cytokine concentrations, the analysis of the results and the writing of the manuscript. I took the lead in organizing the individual steps of the project in consultation with my supervisors and collected joint knowledge. Additionally, I supervised Laura Neumann during her Master thesis who analyzed the immunohistochemical staining. Parts of this study have therefore also been published in her Master's thesis. Prof. Jens Schittenhelm participated in designing the study, data collection, analysis, interpretation as well as critical revision of the manuscript. Evelyn Dubois was involved in data collection and analysis. Dr. Lisa Häsler participated in designing the study and the critical revision of the manuscript. Marius Lambert helped with data collection and analysis of the work. Dr. Mirjam Renovanz contributed to data collection and critical revision of the article. Prof. Gazaleh Tabatabai and Prof. Ulf Ziemann were involved in the critical revision of the manuscript. Prof. Ulrike Naumann contributed to the conception of the study and critically revised the

manuscript. PD Dr. Markus Kowarik was involved in the ethics proposal, conception of the study, development of the experimental design, data interpretation and analysis and critical revision of the manuscript. The individual contributions to this study can also be found online appended to the study [29].

Study 2

The project idea of evaluating B cells in CNS metastases was provided by PD Dr. Markus Kowarik. The methods of single cell sequencing, antibody production, mass sequencing and proteomics analysis have been established and adopted by PD Dr. Markus Kowarik. Proteome and transcriptome analysis was supported by Dr. Gisela Gabernet and the Core Facility for Medical Bioanalytics Tübingen. I strongly contributed to all parts of this project including e.g. ethic approval, tissue request, further method development (especially regarding antigen detection), data acquisition, analysis and inferences. Prof. Ulrike Naumann and PD Dr. Markus Kowarik supervised all experiments. Additionally, I wrote this manuscript. Master student Deniz Bulgur and Bachelor student Célia Hinrichs supported the establishment of an immunohistochemical and immunofluorescence protocol during their theses.

Funding

Parts of this work were funded by the Fortüne Program of the University of Tübingen under grant 2539-0-0. The funding body was not involved in study design, data collection analysis, interpretation nor writing of the manuscript.

References

1. Ostrom QT, Cioffi G, Gittleman H, Patil N, Waite K, Kruchko C, et al. CBTRUS Statistical Report: Primary Brain and Other Central Nervous System Tumors Diagnosed in the United States in 2012–2016. Neuro Oncol. 2019; 21:v1-v100.
2. Qian S, Golubnitschaja O, Zhan X. Chronic inflammation: key player and biomarker-set to predict and prevent cancer development and progression based on individualized patient profiles. EPMA Journal. 2019; 10:365–81.
3. Galdiero MR, Marone G, Mantovani A. Cancer Inflammation and Cytokines. Cold Spring Harb Perspect Biol. 2018; 10:a028662.
4. Greten FR, Grivennikov SI. Inflammation and Cancer: Triggers, Mechanisms, and Consequences. Immunity. 2019; 51:27–41.
5. Dunn GP, Bruce AT, Ikeda H, Old LJ, Schreiber RD. Cancer immunoediting: from immunosurveillance to tumor escape. Nat Immunol. 2002; 3:991–8.

6. Malekghasemi S, Majidi J, Baghbanzadeh A, Abdolalizadeh J, Baradaran B, Aghebati-Maleki L. Tumor-Associated Macrophages: Protumoral Macrophages in Inflammatory Tumor Microenvironment. Adv Pharm Bull. 2020; 10:556–65.
7. Thommen DS, Schumacher TN. T Cell Dysfunction in Cancer. Cancer Cell. 2018; 33:547–62.
8. Fridman WH, Pagès F, Sautès-Fridman C, Galon J. The immune contexture in human tumours: impact on clinical outcome. Nat Rev Cancer. 2012; 12:298–306.
9. Scheper W, Kelderman S, Fanchi LF, Linnemann C, Bendle G, de Rooij, Marije A. J., et al. Low and variable tumor reactivity of the intratumoral TCR repertoire in human cancers. Nat Med. 2019; 25:89–94.
10. Chen DS, Mellman I. Elements of cancer immunity and the cancer–immune set point. Nature. 2017; 541:321–30.
11. Yost KE, Satpathy AT, Wells DK, Qi Y, Wang C, Kageyama R, et al. Clonal replacement of tumor-specific T cells following PD-1 blockade. Nat Med. 2019; 25:1251–9.
12. Xia A, Zhang Y, Xu J, Yin T, Lu X-J. T Cell Dysfunction in Cancer Immunity and Immunotherapy. Front Immunol. 2019; 10:1719.
13. Miggelbrink AM, Jackson JD, Lorrey SJ, Srinivasan ES, Waibl-Polania J, Wilkinson DS, et al. CD4 T-Cell Exhaustion: Does It Exist and What Are Its Roles in Cancer. Clin Cancer Res. 2021; 27:5742-52.
14. Kim SS, Sumner WA, Miyauchi S, Cohen EEW, Califano JA, Sharabi AB. Role of B Cells in Responses to Checkpoint Blockade Immunotherapy and Overall Survival of Cancer Patients. Clin Cancer Res. 2021; 27:6075-82.
15. Jacquelot N,Tellier J, Nutt SI, Belz GT. Tertiary lymphoid structures and B lymphocytes in cancer prognosis and response to immunotherapies. OncoImmunology. 2021; 10:1900508.
16. Wouters MCA, Nelson BH. Prognostic Significance of Tumor-Infiltrating B Cells and Plasma Cells in Human Cancer. Clin Cancer Res. 2018; 24:6125–35.
17. Tokunaga R, Naseem M, Lo JH, Battaglin F, Soni S, Puccini A, et al. B cell and B cell-related pathways for novel cancer treatments. Cancer Treat Rev. 2019; 73:10–9.
18. Kinker GS, Vitiello GAF, Ferreira WAS, Chaves AS, Cordeiro de Lima VC, Medina TdS. B Cell Orchestration of Anti-tumor Immune Responses: A Matter of Cell Localization and Communication. Front Cell Dev Biol. 2021; 9:678127.
19. Zhao K-l, Yang X-j, Jin H-z, Zhao L, Hu J-l, Qin W-j. Double-edge Role of B Cells in Tumor Immunity: Potential Molecular Mechanism. Curr Med Sci. 2019; 39:685–9.
20. Sarvaria A, Madrigal JA, Saudemont A. B cell regulation in cancer and anti-tumor immunity. Cell Mol Immunol. 2017; 14:662–74.
21. Trüb M, Zippelius A. Tertiary Lymphoid Structures as a Predictive Biomarker of Response to Cancer Immunotherapies. Front Immunol. 2021; 12:674565.
22. Singh S, Mehta N, Lilan J, Budhthoki MB, Chao F, Yong L. Initiative action of tumor-associated macrophage during tumor metastasis. Biochim Open. 2017; 4:8–18.
23. Salmaninejad A, Valilou SF, Soltani A, Ahmadi S, Abarghan YJ, Rosengren RJ, et al. Tumor-associated macrophages: role in cancer development and therapeutic implications. Cell Oncol. 2019; 42:591–608.
24. Najafi M, Hashemi Goradel N, Farhood B, Salehi E, Nashtaei MS, Khanlarkhani N, et al. Macrophage polarity in cancer: A review. J Cell Biochem. 2019; 120:2756–65.
25. Laviron M, Boissonnas A. Ontogeny of Tumor-Associated Macrophages. Front Immunol. 2019; 10:1799.
26. Boutilier AJ, Elsawa SF. Macrophage Polarization States in the Tumor Microenvironment. Int J Mol Sci. 2021; 22:6995.
27. Ham S, Lima LG, Lek E, Möller A. The Impact of the Cancer Microenvironment on Macrophage Phenotypes. Front Immunol. 2020; 11:1308.
28. Wang J, Li D, Cang H, Guo B. Crosstalk between cancer and immune cells: Role of tumor-associated macrophages in the tumor microenvironment. Cancer Medicine. 2019; 8:4709–21.

29. Kemmerer CL, Schittenhelm J, Dubois E, Neumann L, Häsler LM, Lambert M, et al. Cerebrospinal fluid cytokine levels are associated with macrophage infiltration into tumor tissues of glioma patients. BMC cancer. 2021; 21:1108.
30. Stupp R, Taillibert S, Kanner A, Read W, Steinberg DM, Lhermitte B, et al. Effect of Tumor-Treating Fields Plus Maintenance Temozolomide vs Maintenance Temozolomide Alone on Survival in Patients With Glioblastoma. JAMA. 2017; 318:2306-16.
31. Yao M, Li S, Wu X, Diao S, Zhang G, He H, et al. Cellular origin of glioblastoma and its implication in precision therapy. Cell Mol Immunol. 2018; 15:737–9.
32. Louis DN, Perry A, Reifenberger G, Deimling A von, Figarella-Branger D, Cavenee WK, et al. The 2016 World Health Organization Classification of Tumors of the Central Nervous System: a summary. Acta Neuropathol. 2016; 131:803–20.
33. Wang H, Zhou H, Xu J, Lu Y, Ji X, Yao Y, et al. Different T-cell subsets in glioblastoma multiforme and targeted immunotherapy. Cancer Letters. 2021; 496:134–43.
34. Mohme M, Neidert MC. Tumor-Specific T Cell Activation in Malignant Brain Tumors. Front Immunol. 2020; 11:205.
35. Grabowski MM, Sankey EW, Ryan KJ, Chongsathidkiet P, Lorrey SJ, Wilkinson DS, et al. Immune suppression in gliomas. J Neurooncol. 2021; 151:3–12.
36. Ooi YC, Tran P, Ung N, Thill K, Trang A, Fong BM, et al. The role of regulatory T-cells in glioma immunology. Clin Neurol Neurosurg. 2014; 119:125–32.
37. Lee-Chang C, Rashidi A, Miska J, Zhang P, Pituch KC, Hou D, et al. Myeloid-Derived Suppressive Cells Promote B cell-Mediated Immunosuppression via Transfer of PD-L1 in Glioblastoma. Cancer Immunol Res. 2019; 7:1928–43.
38. Orrego E, Castaneda CA, Castillo M, Bernabe LA, Casavilca S, Chakravarti A, et al. Distribution of tumor-infiltrating immune cells in glioblastoma. CNS Oncol. 2018; 7:CNS21.
39. Domingues P, González-Tablas M, Otero Á, Pascual D, Miranda D, Ruiz L, et al. Tumor infiltrating immune cells in gliomas and meningiomas. Brain Behav, Immun. 2016; 53:1-15
40. Lee-Chang C, Miska J, Hou D, Rashidi A, Zhang P, Burga RA, et al. Activation of 4-1BBL+ B cells with CD40 agonism and IFNγ elicits potent immunity against glioblastoma. J Exp Med. 2021; 218:e20200913.
41. Wei J, Chen P, Gupta P, Ott M, Zamler D, Kassab C, et al. Immune biology of glioma associated macrophages and microglia: Functional and therapeutic implications. Neuro-Oncology. 2019; 22: 180-94
42. Guadagno E, Presta I, Maisano D, Donato A, Pirrone C, Cardillo G, et al. Role of Macrophages in Brain Tumor Growth and Progression. Int J Mol Sci. 2018; 19:1005.
43. Grégoire H, Roncali L, Rousseau A, Chérel M, Delneste Y, Jeannin P, et al. Targeting Tumor Associated Macrophages to Overcome Conventional Treatment Resistance in Glioblastoma. Front Pharmacol. 2020; 11:368.
44. Vidyarthi A, Agnihotri T, Khan N, Singh S, Tewari MK, Radotra BD, et al. Predominance of M2 macrophages in gliomas leads to the suppression of local and systemic immunity. Cancer Immunol Immunother. 2019; 68:1995–2004.
45. Chen Z, Feng X, Herting CJ, Garcia VA, Nie K, Pong WW, et al. Cellular and Molecular Identity of Tumor-Associated Macrophages in Glioblastoma. Cancer Res. 2017; 77:2266–78.
46. Müller S, Kohanbash G, Liu SJ, Alvarado B, Carrera D, Bhaduri A, et al. Single-cell profiling of human gliomas reveals macrophage ontogeny as a basis for regional differences in macrophage activation in the tumor microenvironment. Genome Biol. 2017; 18:234.
47. Quail DF, Joyce JA. The Microenvironmental Landscape of Brain Tumors. Cancer Cell. 2017; 31:326–41.
48. Pires-Afonso Y, Niclou SP, Michelucci A. Revealing and Harnessing Tumour-Associated Microglia/Macrophage Heterogeneity in Glioblastoma. Int J Mol Sci. 2020; 21:689.

49. Gjorgjevski M, Hannen R, Carl B, Li Y, Landmann E, Buchholz M, et al. Molecular profiling of the tumor microenvironment in glioblastoma patients: correlation of microglia/macrophage polarization state with metalloprotease expression profiles and survival. Biosci Rep. 2019; 39:BSR20182361.
50. dello Russo C, Lisi L, Tentori L, Navarra P, Graziani G, Combs C. Exploiting Microglial Functions for the Treatment of Glioblastoma. Current Cancer Drug Targets. 2017; 17:267–81.
51. Yeo ECF, Brown MP, Gargett T, Ebert LM. The Role of Cytokines and Chemokines in Shaping the Immune Microenvironment of Glioblastoma: Implications for Immunotherapy. Cells. 2021; 10:607.
52. Iwami K, Natsume A, Wakabayashi T. Cytokine networks in glioma. Neurosurg Rev. 2011; 34:253–64.
53. Zhu VF, Yang J, Lebrun DG, Li M. Understanding the role of cytokines in Glioblastoma Multiforme pathogenesis. Cancer Letters. 2012; 316:139–50. Epub 2011/11/07.
54. Gieryng A, Pszczolkowska D, Walentynowicz KA, Rajan WD, Kaminska B. Immune microenvironment of gliomas. Lab Invest. 2017; 97:498–518.
55. Jordan JT, Sun W, Hussain SF, DeAngulo G, Prabhu SS, Heimberger AB. Preferential migration of regulatory T cells mediated by glioma-secreted chemokines can be blocked with chemotherapy. Cancer Immunol Immunother. 2008; 57:123–31.
56. Iwadate Y, Namba H, Sakiyama S, Yamaura A, Tagawa M. Interleukin-12-mediated induction of systemic immunity in the periphery and recruitment of activated T cells into the brain produce limited antitumor effects compared with interleukin-2. Int J Mol Med. 2002; 10:741–7.
57. Lohr L, Ratliff T, Huppertz A, Ge Y, Dictus C, Ahmadi R, et al. Effector T-Cell Infiltration Positively Impacts Survival of Glioblastoma Patients and Is Impaired by Tumor-Derived TGF-β. Clin Cancer Res. 2011; 17:4296–308.
58. Liau LM, Prins RM, Kiertscher SM, Odesa SK, Kremen TJ, Giovannone AJ, et al. Dendritic Cell Vaccination in Glioblastoma Patients Induces Systemic and Intracranial T-cell Responses Modulated by the Local Central Nervous System Tumor Microenvironment. Clin Cancer Res. 2005; 11:5515–25.
59. Chang AL, Miska J, Wainwright DA, Dey M, Rivetta CV, Yu D, et al. CCL2 produced by the glioma microenvironment is essential for the recruitment of regulatory T cells and myeloid-derived suppressor cells. Cancer Res. 2016; 76:5671–82.
60. Krzyszkowski T, Dziedzic T, Czepko R, Szczudlik A. Decreased levels of interleukin-10 and transforming growth factor-beta 2 in cerebrospinal fluid of patients with high grade astrocytoma. Neurol Res. 2008; 30:294-6.
61. Lepennetier G, Hracsko Z, Unger M, van Griensven M, Grummel V, Krumbholz M, et al. Cytokine and immune cell profiling in the cerebrospinal fluid of patients with neuro-inflammatory diseases. J Neuroinflammation. 2019; 16:219.
62. Mauri C, Menon M. Human regulatory B cells in health and disease: therapeutic potential. J Clin Invest. 2017; 127:772–9.
63. Balik V, Mirossay P, Bohus P, Sulla I, Mirossay L, Sarissky M. Flow Cytometry Analysis of Neural Differentiation Markers Expression in Human Glioblastomas May Predict Their Response to Chemotherapy. Cell Mol Neurobiol. 2009; 29:845–58.
64. Pinton L, Masetto E, Vettore M, Solito S, Magri S, D'Andolfi M, et al. The immune suppressive microenvironment of human gliomas depends on the accumulation of bone marrow-derived macrophages in the center of the lesion. J Immunotherapy Cancer. 2019; 7:58..
65. Liebner S, Dijkhuizen RM, Reiss Y, Plate KH, Agalliu D, Constantin G. Functional morphology of the blood–brain barrier in health and disease. Acta Neuropathol. 2018; 135:311–36.
66. Brandenburg S, Müller A, Turkowski K, Radev YT, Rot S, Schmidt C, et al. Resident microglia rather than peripheral macrophages promote vascularization in brain tumors and are source of alternative pro-angiogenic factors. Acta Neuropathol. 2016; 131:365–78.

67. Zhu C, Kros JM, van dWM, Zheng P, Cheng C, Mustafa DA. Expression site of P2RY12 in residential microglial cells in astrocytomas correlates with M1 and M2 marker expression and tumor grade. Acta Neuropathol Commun. 2017; 5:4.
68. Pathangey LB, McCurry DB, Gendler SJ, Dominguez AL, Gorman JE, Pathangey G, et al. Surrogate in vitro activation of innate immunity synergizes with interleukin-7 to unleash rapid antigen-driven outgrowth of CD4+ and CD8+ human peripheral blood T-cells naturally recognizing MUC1, HER2/neu and other tumor-associated antigens. Oncotarget. 2017; 8:10785-808.
69. Tan JT, Dudl E, LeRoy E, Murray R, Sprent J, Weinberg KI, et al. IL-7 is critical for homeostatic proliferation and survival of naive T cells. Proc Natl Acad Sci U S A. 2001; 98:8732–7.
70. Gao J, Zhao L, Wan YY, Zhu B. Mechanism of Action of IL-7 and Its Potential Applications and Limitations in Cancer Immunotherapy. Int J Mol Sci. 2015; 16:10267–80.
71. Fritzell S, Eberstål S, Sandén E, Visse E, Darabi A, Siesjö P. IFNγ in combination with IL-7 enhances immunotherapy in two rat glioma models. J Neuroimmunol. 2013; 258:91–5.
72. Shan Y, He X, Song W, Han D, Niu J, Wang J. Role of IL-6 in the invasiveness and prognosis of glioma. Int J Clin Exp Med. 2015; 8:9114-20.
73. Vera S, Sinning M, Vergara M, Lemus D, Rosas C. Cerebrospinal fluid VEGF levels and angiogenic capacity as potential prognostic markers in patients with gliomas: a pilot study. J Neurooncol. 2019; 145:233–9.
74. Sampath P, Weaver CE, Sungarian A, Cortez S, Alderson L, Stopa EG. Cerebrospinal fluid (vascular endothelial growth factor) and serologic (recoverin) tumor markers for malignant glioma. Cancer Control. 2004; 11:174–80.
75. Peles E, Lidar Z, Simon AJ, Grossman R, Nass D, Ram Z. Angiogenic Factors in the Cerebrospinal Fluid of Patients with Astrocytic Brain Tumors. Neurosurgery. 2004; 55:562–8.
76. Hori T, Sasayama T, Tanaka K, Koma Y-i, Nishihara M, Tanaka H, et al. Tumor-associated macrophage related interleukin-6 in cerebrospinal fluid as a prognostic marker for glioblastoma. J Clin Neurosci. 2019; 68:281–9.
77. Berghoff AS, Ricken G, Widhalm G, Rajky O, Dieckmann K, Birner P, et al. Tumour-infiltrating lymphocytes and expression of programmed death ligand 1 (PD-L1) in melanoma brain metastases. Histopathology. 2015; 66:289–99.
78. Berghoff AS, Ricken G, Wilhelm D, Rajky O, Widhalm G, Dieckmann K, et al. Tumor infiltrating lymphocytes and PD-L1 expression in brain metastases of small cell lung cancer (SCLC). J Neurooncol. 2016; 130:19–29.
79. Shapouri-Moghaddam A, Mohammadian S, Vazini H, Taghadosi M, Esmaeili S-A, Mardani F, et al. Macrophage plasticity, polarization, and function in health and disease. J Cell Physiol. 2018; 233:6425–40.
80. Jiménez AJ, Domínguez-Pinos M-D, Guerra MM, Fernández-Llebrez P, Pérez-Fígares J-M. Structure and function of the ependymal barrier and diseases associated with ependyma disruption. Tissue Barriers. 2014; 2:e28426.
81. Binabaj MM, Bahrami A, ShahidSales S, Joodi M, Joudi Mashhad M, Hassanian SM, et al. The prognostic value of MGMT promoter methylation in glioblastoma: A meta-analysis of clinical trials. J Cell Physiol. 2018; 233:378–86.
82. Ostrand-Rosenberg S. Immune surveillance: a balance between protumor and antitumor immunity. Curr Opin Genet Dev. 2008; 18:11–8.
83. Albulescu R, Codrici E, Popescu ID, Mihai S, Necula LG, Petrescu D, et al. Cytokine Patterns in Brain Tumour Progression. Mediators Inflamm. 2013; 2013:979748.
84. YT Yeung, KL McDonald, T Grewal, L Munoz. Interleukins in glioblastoma pathophysiology: implications for therapy. Br J Pharmacol. 2013; 168:591–606.
85. Zeiner PS, Preusse C, Golebiewska A, Zinke J, Iriondo A, Muller A, et al. Distribution and prognostic impact of microglia/macrophage subpopulations in gliomas. Brain Pathol. 2019; 29:513–29.

86. Mignogna C, Signorelli F, Vismara MFM, Zeppa P, Camastra C, Barni T, et al. A reappraisal of macrophage polarization in glioblastoma: Histopathological and immunohistochemical findings and review of the literature. Pathol Res Pract. 2016; 212:491–9.
87. Engelhardt B, Vajkoczy P, Weller RO. The movers and shapers in immune privilege of the CNS. Nat Immunol. 2017; 18:123–31.
88. Zewde M, Kiyotani K, Park J-H, Fang H, Yap KL, Yew PY, et al. The era of immunogenomics/immunopharmacogenomics. J Hum Genet. 2018; 63:865–75.
89. Simon JS, Botero S, Simon SM. Sequencing the peripheral blood B and T cell repertoire – Quantifying robustness and limitations. J Immunol Methods. 2018; 463:137–47.
90. Konishi H, Komura D, Katoh H, Atsumi S, Koda H, Yamamoto A, et al. Capturing the differences between humoral immunity in the normal and tumor environments from repertoire-seq of B-cell receptors using supervised machine learning. BMC bioinformatics. 2019; 20:267.
91. Song L, Ouyang Z, Cohen D, Cao Y, Altreuter J, Bai G, et al. Comprehensive Characterizations of Immune Receptor Repertoire in Tumors and Cancer Immunotherapy Studies. Cancer Immunol Res. 2022; 10:788–99.
92. Dunn-Walters D, Townsend C, Sinclair E, Stewart A. Immunoglobulin gene analysis as a tool for investigating human immune responses. Immunol Rev. 2018; 284:132–47.
93. Zhang P, Chou H-Y, Young L, Zheng P, Liu Y. En masse discovery of anti-cancer human monoclonal antibodies by de novo assembly of immunoglobulin sequences from transcriptomes and genome sequences of cancer tissues. Cell Mol Immunol. 2019; 16:943–5.
94. Canzar S, Neu KE, Tang Q, Wilson PC, Khan AA. BASIC: BCR assembly from single cells. Bioinformatics. 2017; 33:425-7.
95. See P, Lum J, Chen J, Ginhoux F. A Single-Cell Sequencing Guide for Immunologists. Front Immunol. 2018; 9:2425.
96. Kowarik MC, Grummel V, Wemlinger S, Buck D, Weber MS, Berthele A, et al. Immune cell subtyping in the cerebrospinal fluid of patients with neurological diseases. J Neurol. 2014; 261:130–43.
97. Deutsche Gesellschaft für Neurologie, V. LL 77 Hirnmetastasen und Meningeosis neoplastica - Deutsche Gesellschaft für Neurologie [updated 16 Oct 2020+00:00; cited 3 Mar 2022.781Z]. Available from: https://dgn.org/leitlinien/ll-77-hirnmetastasen-und-meningeos-neoplastica/.
98. Djukic M, Trimmel R, Nagel I, Spreer A, Lange P, Stadelmann C, et al. Cerebrospinal fluid abnormalities in meningeosis neoplastica: a retrospective 12-year analysis. Fluids Barriers CNS. 2017; 14:7.
99. Wennhold K, Thelen M, Lehmann J, Schran S, Preugszat E, Garcia-Marquez M, et al. CD86+ Antigen-Presenting B Cells Are Increased in Cancer, Localize in Tertiary Lymphoid Structures, and Induce Specific T-cell Responses. Cancer Immunol Res. 2021; 9:1098–108.
100. de Jonge H, Iamele L, Maggi M, Pessino G, Scotti C. Anti-Cancer Auto-Antibodies: Roles, Applications and Open Issues. Cancers (Basel). 2021; 13:813.
101. Mou Z, He Y, Wu Y. Immunoproteomics to identify tumor-associated antigens eliciting humoral response. Cancer Letters. 2009; 278:123–9.
102. Ganesan V, Ascherman DP, Minden JS. Immunoproteomics technologies in the discovery of auto-antigens in autoimmune diseases. Biomol Concepts. 2016; 7:133–43.
103. DeFalco J, Harbell M, Manning-Bog A, Baia G, Scholz A, Millare B, et al. Non-progressing cancer patients have persistent B cell responses expressing shared antibody paratopes that target public tumor antigens. Clin Immunol. 2018; 187:37–45.
104. Rodriguez-Pinto D, Sparkowski J, Keough MP, Phoenix KN, Vumbaca F, Han DK, et al. Identification of novel tumor antigens with patient-derived immune-selected antibodies. Cancer Immunol Immunother. 2009; 58:221–34.

105. Pavoni E, Monteriù G, Santapaola D, Petronzelli F, Anastasi AM, Pelliccia A, et al. Tumor-infiltrating B lymphocytes as an efficient source of highly specific immunoglobulins recognizing tumor cells. BMC Biotechnol. 2007; 7:1–17.
106. Bushey RT, Moody MA, Nicely NL, Haynes BF, Alam SM, Keir ST, et al. A Therapeutic Antibody for Cancer, Derived from Single Human B Cells. Cell Reports. 2016; 15:1505–13.
107. Owens GP, Ritchie AM, Burgoon MP, Williamson RA, Corboy JR, Gilden DH. Single-Cell Repertoire Analysis Demonstrates that Clonal Expansion Is a Prominent Feature of the B Cell Response in Multiple Sclerosis Cerebrospinal Fluid. J Immunol. 2003; 171:2725–33.
108. Retter I, Althaus HH, Münch R, Müller W. VBASE2, an integrative V gene database. Nucleic Acids Res. 2005; 33:D671-4.
109. Kowarik MC, Astling D, Gasperi C, Wemlinger S, Schumann H, Dzieciatkowska M, et al. CNS Aquaporin-4-specific B cells connect with multiple B-cell compartments in neuromyelitis optica spectrum disorder. Ann Clin Transl Neurol. 2017; 4:369–80.
110. Brochet X, Lefranc MP, Giudicelli V. IMGT/V-QUEST: the highly customized and integrated system for IG and TR standardized V-J and V-D-J sequence analysis. Nucleic acids research. 2008; 36:W503-8.
111. Ruschil C, Gabernet G, Lepennetier G, Heumos S, Kaminski M, Hracsko Z, et al. Specific Induction of Double Negative B Cells During Protective and Pathogenic Immune Responses. Front Immunol. 2020; 11:606338.
112. The Human Protein Atlas [updated 12 May 2022.000Z; cited 12 May 2022.674Z]. Available from: https://www.proteinatlas.org/about/licence.
113. Uhlen M, Zhang C, Lee S, Sjöstedt E, Fagerberg L, Bidkhori G, et al. A pathology atlas of the human cancer transcriptome. Science. 2017; 357:eaan2507.
114. Saul L, Ilieva KM, Bax HJ, Karagiannis P, Correa I, Rodriguez-Hernandez I, et al. IgG subclass switching and clonal expansion in cutaneous melanoma and normal skin. Sci Rep. 2016; 6:29736.
115. Barrow C, Browning J, MacGregor D, Davis ID, Sturrock S, Jungbluth AA, et al. Tumor Antigen Expression in Melanoma Varies According to Antigen and Stage. Clin Cancer Res. 2006; 12:764–71.
116. S. Yamada, H. Ito, M. Ishikawa, K. Yamamoto, M. Yamaguchi, M. Oshima, et al. Quantification of Oscillatory Shear Stress from Reciprocating CSF Motion on 4D Flow Imaging. Am J Neuroradiol. 2021; 42:479.
117. Galluzzi L, Buqué A, Kepp O, Zitvogel L, Kroemer G. Immunogenic cell death in cancer and infectious disease. Nat Rev Immunol. 2017; 17:97–111.
118. Wang, Y., Liu, J., Burrows, P.D., Wang, JY. (2020). B Cell Development and Maturation. In: Wang, JY. (eds) B Cells in Immunity and Tolerance. Advances in Experimental Medicine and Biology, vol 1254. Springer, Singapore.
119. Owens GP, Shearer AJ, Yu X, Ritchie AM, Keays KM, Bennett JL, et al. Screening Random Peptide Libraries with Subacute Sclerosing Panencephalitis Brain-Derived Recombinant Antibodies Identifies Multiple Epitopes in the C-Terminal Region of the Measles Virus Nucleocapsid Protein. Journal of Virology. 2006; 80:12121-30.
120. Dunbar J, Krawczyk K, Leem J, Marks C, Nowak J, Regep C, et al. SAbPred: a structure-based antibody prediction server. Nucleic Acids Res. 2016; 44:W474-8.
121. Krawczyk K, Liu X, Baker T, Shi J, Deane CM. Improving B-cell epitope prediction and its application to global antibody-antigen docking. Bioinformatics. 2014; 30:2288–94.
122. Dondelinger M, Filée P, Sauvage E, Quinting B, Muyldermans S, Galleni M, et al. Understanding the Significance and Implications of Antibody Numbering and Antigen-Binding Surface/Residue Definition. Front Immunol. 2018; 9:2278.
123. Fernández-Quintero ML, Loeffler JR, Bacher LM, Waibl F, Seidler CA, Liedl KR. Local and Global Rigidification Upon Antibody Affinity Maturation. Front Mol Biosci. 2020; 7:182.

124. Manivel V, Sahoo NC, Salunke DM, Rao KV. Maturation of an antibody response is governed by modulations in flexibility of the antigen-combining site. Immunity. 2000; 13:611-20.
125. Breden F, Lepik C, Longo NS, Montero M, Lipsky PE, Scott JK. Comparison of Antibody Repertoires Produced by HIV-1 Infection, Other Chronic and Acute Infections, and Systemic Autoimmune Disease. PLOS ONE. 2011; 6:e16857.
126. Barrios Y, Jirholt P, Ohlin M. Length of the antibody heavy chain complementarity determining region 3 as a specificity-determining factor. J Mol Recognit. 2004; 17:332–8.
127. Collis AVJ, Brouwer AP, Martin ACR. Analysis of the Antigen Combining Site: Correlations Between Length and Sequence Composition of the Hypervariable Loops and the Nature of the Antigen. J Mol Bio. 2003; 325:337–54.
128. Chen D, Zhang Z, Yang Y, Hong Q, Li W, Zhuo L. High-throughput sequencing analysis of genes encoding the B-lymphocyte receptor heavy-chain CDR3 in renal and peripheral blood of IgA nephropathy. Biosci Rep. 2019; 39:BSR20190482.
129. Imkeller K, Wardemann H. Assessing human B cell repertoire diversity and convergence. Immunol Rev. 2018; 284:51–66.
130. van Tongelen A, Loriot A, Smet C de. Oncogenic roles of DNA hypomethylation through the activation of cancer-germline genes. Cancer Letters. 2017; 396:130–7.
131. Kim H, Kim Y, Jeoung D. DDX53 Promotes Cancer Stem Cell-Like Properties and Autophagy. Molecules and cells. 2017; 40:54-65.
132. Kim Y, Yeon M, Jeoung D. DDX53 Regulates Cancer Stem Cell-Like Properties by Binding to SOX-2. Molecules and cells. 2017; 40:322-30.
133. Meistere I, Werner S, Zayakin P, Siliņa K, Rulle U, Pismennaja A, et al. The Prevalence of Cancer-Associated Autoantibodies in Patients with Gastric Cancer and Progressive Grades of Premalignant Lesions. Cancer Epidemiol Biomarkers Prev. 2017; 26:1564–74.
134. Pongor L, Kormos M, Hatzis C, Pusztai L, Szabó A, Győrffy B. A genome-wide approach to link genotype to clinical outcome by utilizing next generation sequencing and gene chip data of 6,697 breast cancer patients. Genome Med. 2015; 7:104.
135. https://www.healthtech.dtu.dk. Services [updated 18 Aug 2022.000Z; cited 18 Aug 2022.404Z]. Available from: https://services.healthtech.dtu.dk/service.php?NetNGlyc-1.0.
136. Lam CWK, Chui SH, Leung NWY, Li EKM, Lai KN. Light chain ratios of serum immunoglobulins in disease. Clin Biochem. 1991; 24:283–7.
137. Peuscher A, Gassler N, Schneider U, Thom P, Rasche S, Spiegel H, et al. An immunohistochemical assay on human tissue using a human primary antibody. J Immunoassay Immunochem. 2014; 35:322–34.
138. Goodpaster T, Randolph-Habecker J. A flexible mouse-on-mouse immunohistochemical staining technique adaptable to biotin-free reagents, immunofluorescence, and multiple antibody staining. J Histochem Cytochem. 2014; 62:197–204.
139. Veomett N, Dao T, Scheinberg DA. Therapeutic antibodies to intracellular targets in cancer therapy. Expert Opin Biol Ther. 2013; 13:1485–8.
140. Nagayama A, Ellisen LW, Chabner B, Bardia A. Antibody–Drug Conjugates for the Treatment of Solid Tumors: Clinical Experience and Latest Developments. Targ Oncol. 2017; 12:719–39.
141. Page A, Hubert J, Fusil F, Cosset F-L. Exploiting B Cell Transfer for Cancer Therapy: Engineered B Cells to Eradicate Tumors. Int J Mol Sci. 2021; 22:9991.
142. Moutai T, Yamana H, Nojima T, Kitamura D. A Novel and Effective Cancer Immunotherapy Mouse Model Using Antigen-Specific B Cells Selected In Vitro. PLOS ONE. 2014; 9:e92732.
143. Buonaguro L, Tagliamonte M. Selecting Target Antigens for Cancer Vaccine Development. Vaccines. 2020; 8:615.